Rainfall Redistribution by the Canopy of a Juvenile Lodgepole Pine Stand

by

Chad Edward Lishman

B.A. Thompson Rivers University, 2009

P.Ag., British Columbia Institute of Agrology, 2013

A THESIS SUBMITTED IN PARTIAL FULFILLMENT OF

THE REQUIREMENTS FOR THE DEGREE OF

MASTER OF SCIENCE (ENVIRONMENTAL SCIENCE)

Thompson Rivers University
Kamloops, British Columbia, Canada
September, 2015

Thesis examining committee:

Darryl Carlyle-Moses (PhD), Thesis Supervisor and Associate Professor and Chair, Department of Geography & Environmental Studies, Thompson Rivers University

David Hill (PhD), Associate Professor and Committee Member, Department of Geography & Environmental Studies, Thompson Rivers University

Thomas G Pypker (PhD), Assistant Professor and Committee Member, Department of Natural Resource Science, Thompson Rivers University

Rita Winkler (PhD, R.P.F.), Research Hydrologist, British Columbia Ministry of Forests, Lands and Natural Resource Operations

Delphis Levia (PhD), External Reader, Professor of Ecohydrology and Director, Environmental Science and Environmental Studies, Department of Geography, University of Delaware

Thesis Supervisor: Dr. Darryl Carlyle-Moses

ABSTRACT

From May to October 2010, throughfall associated with 38 rainfall events in three below-canopy zones (inner-canopy, mid-canopy, and canopy-periphery) of nine juvenile lodgepole pine trees and in open areas between canopies was measured along north, south, east and west transects radiating from each tree bole. Median cumulative throughfall (%) significantly differed among the canopy zones under differing rain depth classes and was negatively correlated with tree size metrics, but only for certain combinations of canopy zones and rain depth classes. Although median cumulative throughfall (%) was negatively correlated with canopy cover fraction when all below-canopy gauges were considered, this relationship only held true for the inner- and mid-canopy zones under relatively small rain depth classes. Additionally, cumulative throughfall (%) was often dependent on transect direction, with event throughfall showing a dependence on the direction of storm origin. Temporal persistence of throughfall was assessed using time stability plots and Spearman rank coefficients of rain event and depth class pairings for all gauges and by canopy zone. The influence of temporal lag and meteorological variables on persistence was also assessed. The implications of our findings on throughfall sampling and for future ecohydrological studies in juvenile lodgepole pine and similar stands are discussed. Additionally, stemflow was measured so that a full canopy water balance could be derived for each event and over the study period. Canopy interception loss, throughfall and stemflow accounted for 87.7, 10.5, and 1.8% of the study-period rainfall, respectfully. Both the reformulated Gash and reformulated Liu models were found to have satisfactory simulated study-period interception loss; however, estimates at the rain-event scale were often poor. Interception loss from the juvenile stand is largely a factor of canopy cover fraction and relatively high during-rainfall evaporation rates.

TABLE OF CONTENTS

LIST OF TABLES

LIST OF FIGURES

LIST OF SYMBOLS

A – Total Area beneath the tree canopy

a – Slope

a_z – Area of the below canopy zone

BA – Basal area

BC – British Columbia

CPA – Crown projection area

DOSO – Direction of Storm Orgin

F – Funnelling ratio

Ha – Hectare

Ic – Interception Loss

MPB – Mountain Pine Beetle

P_A – Annual rainfall

P_d – Drainage partitioning coefficient

PCA – Projected Crown Area

P_g – Incident precipitation falling on the canopy

P_g' – Canopy storage capacity

P_g '' – Trunk Storage Capacity

R – Incident precipitation

S – Canopy Storage Capacity

SF – Stemflow

S_t – Trunk Storage Capacity

TF – Throughfall

TF_T – Total below canopy throughfall

TF_z – Mean throughfall catch within the below canopy zone

ACKNOWLEDGEMENTS

I owe my deepest gratitude to my supervisor, Dr. Darryl Carlyle-Moses, for encouraging me to join the Masters of Science program at TRU and for his continuous support, participation, expertise and guidance that made the completion of this thesis conceivable. Thank you for my thesis committee, Dr. Rita Winkler, Dr. David Hill, and Dr. Delphis Levia, for their patience, time and direction. Thank you for my research crew, Pearce Sanders, Andrew Pillar, Jenn Golden, and Adam McKee, for their extraordinary effort, countless hours and support.

This thesis would not have been possible without the funding support awarded to Dr. Darryl Carlyle-Moses, provided by the NSERC (Natural Sciences and Engineering Research Council of Canada) Discovery Grant and the FIA-FSP (Forest Investment Account – Forest Science Program).

I would like to thank my family and friends for their support over the past few years that have helped push me to complete this thesis, and especially to Jenna Lishman who continues to push me forward.

CHAPTER 1
INTRODUCTION

Lodgepole pine (*Pinus contorta* var. *latifolia* Dougl) forests of the central interior region of British Columbia are habitats which are under constant threat from extensive forest fires, mountain pine beetle (MPB) outbreaks, logging, grazing and range land encroachment (B.C. Ministry of Forests, Mines and Lands. 2010). This area plays a crucial role in being the headwaters for many of the regions creeks and rivers. With the recent MPB outbreak, 10.1 million ha of lodgepole pine forests were affected, which resulted in increased harvesting, salvaging and planting in the region (Axelson *et al*., 2009). As a result, juvenile lodgepole pine stands are becoming increasingly dominant in the region, replacing the harvested, or deceased mature stands. Numerous studies have been conducted in British Columbia and around the world regarding rainfall interception; however they have been primarily focused on mature forests (Spittlehouse, 1998). Thus, for a better understanding of the hydrological effects of the transition from a mature forest to a juvenile forest dominated landscape, rainfall interception and the interaction between near-surface soil moisture and the atmospheric boundary layer must be studied.

Spatial delivery of precipitation from the tree canopy to the soil occurs through two processes, throughfall and stemflow. Throughfall and stemflow are usually calculated as the difference between incident gross precipitation and interception. In temperate forests, stemflow and throughfall typically account for 70-90% of the incident gross precipitation (Levia and Frost, 2003). The bulk of understory precipitation, however, reaches the forest floor in the form of throughfall. At the stand scale, throughfall commonly represents > 90% of the understory precipitation input (Brabender, 2005). The spatial variability of throughfall is not inconsequential. Price et al. (1997), for example, found that the spatial variability of throughfall, expressed as a coefficient of variation (CV), in a black spruce (*Picea mariana*) stand decreased asymptotically with rainstorm size, averaging 60% of rainfall for ‘small’ events and 24% for ‘large’ rainfalls (> 10 mm). Although the spatial variability of throughfall is a consequence of rainfall interacting with the canopy, the interactions that occur and the resulting throughfall spatial pattern, or lack thereof, appear to be ecosystem dependent (e.g., Loustau *et al*. 1992; Carlyle-Moses *et al*., 2004; Nadkarni and Sumera, 2004). Determining if throughfall input is random or if it is systematically related to stand

characteristics (e.g., distance from the tree bole) is an important consideration for the proper estimation of throughfall input to the forest floor and for soil moisture variability.

Some researchers have found that there is no spatial correlation in forest throughfall (Laostau *et al*. 1992; Bellot and Escarre, 1998), while others have found evidence of spatial autocorrelation (Loescher *et al*. 2002; Gomez *et al*. 2002). Keim *et al*. (2005) concluded that throughfall spatial correlation was highly variable and differed depending on type of stand and season, which yielded results of no correlation in some stands to correlation lengths from 3-10 m in others.

In a mixed deciduous forest in Belgium, Staelens *et al*. (2006) conducted a spatial and temporal throughfall variability study to determine if there were any spatial patterns. They concluded that during the leafed periods, throughfall was spatially correlated up to a distance of 3-4 m. In addition, they determined that there was considerable temporal stability of the spatial throughfall pattern in the growing season and the dormant period. Furthermore, throughfall water during the growing season drastically decreased with increasing canopy cover, and was determined to be closely correlated with branch cover; however, the spatial pattern of throughfall in the dormant period was not related to the branch cover.

The distance over which throughfall is correlated is determined by stand characteristics such as tree species, stand density, and canopy structure (Keim *et al*., 2005). However, it is difficult to compare the spatial correlation lengths and patterns (or lack thereof) of throughfall between one stand and another, due, in large part, to the multitude of factors that affect throughfall, such as tree geometry, basal area, tree density, age, understory abundance, crown cover, season, and numerous other variables (Huber and Iroumé, 2001).

When compared to throughfall, stemflow inputs to the forest floor have a greater spatial variability and are more concentrated (Levia, and Frost, 2003). With the high spatial variability of stemflow, Tanka *et al*. (1996) proposed that the actual amount of stemflow infiltrating in a circular pattern around the tree trunk may represent as much as 10-20% of the incident gross precipitation, which results in soil moisture and ground water recharge. As mentioned, the spatial variability of stemflow is large, controlled in part, by wind, rain intensity and duration, crown projection area, tree density, age, branch inclination and species type (Levia and Frost 2003). Another factor influencing stemflow is angled rainfall (Van Stan *et al*., 2011). Due to wind, most rain events do not fall vertically but on an angle.

This creates uneven interception due to taller trees causing a partial or full rainshadow on neighbouring trees, which causes uneven stemflow production, with the taller trees producing a greater volume than the rain shadowed trees (Levia and Frost, 2003). In general the spatial variability of stemflow generation decreases as the magnitude of a precipitation event increases (Levia and Frost, 2003).

Stemflow typically accounts for 5 to 10% of the gross precipitation in most forest environments. (Levia and Frost, 2003; Li et al., 2008; Tanaka et al.,1996; Taniguchi et al., 1996). However, in mature coniferous forests stemflow is typically a negligible (< 1% of precipitation) component of forest water balance (Price et al., 1997; Spittlehouse, 1998). Since stemflow accounts for only a few percent of the gross precipitation, many studies have ignored its hydrological significance. However, the volume of water delivered to the base of trees may be very large, far exceeding rainfall and throughfall inputs on a per unit area basis (Murakami, 2009). Herwitz (1986) introduced a metric for quantitatively describing the importance of stemflow as a point input. This *funneling ratio* is found as:

$$F = \frac{SF_{vol.}}{P_g \cdot BA} \tag{1.1}$$

where F is the funneling ratio (dimensionless), $SF_{vol.}$ is the stemflow volume (litres), P_g is gross precipitation and BA represents the tree basal area (m^2).

The stemflow funneling ratio represents the amount of water delivered to the base of the tree compared to that which would be captured by an unobstructed rain gauge having an orifice area equal to the tree BA. Thus, F values > 1 indicate that portions of the tree canopy outside of the tree bole are contributing to stemflow.

Most published F values are from either semi-arid or tropical rainforest environments. Funneling ratios from these studies have been found to be highly variable, ranging from 2 for an individual mesquite (*Prosopis laevigata*) tree in northeastern Mexico (Navar and Bryan, 1990) to 276 for an individual Sierra palm (*Prestoea montana*) in Puerto Rico (Holwerda et al., 2006, as calculated by McKee, 2010). The only study to be conducted in a temperate deciduous forest during growing season conditions (Carlyle-Moses and Price, 2006) found that geometric mean F values were 7.3, 20.6 and 26.3 for red oak (*Quercus*

rubra), sugar maple (*Acer saccharum*) and American beech (*Fagus grandifolia*), respectively. No known studies have reported *F* values for mature coniferous forests; however, McKee and Carlyle-Moses (2010) found that funneling ratios for juvenile lodgepole pine during a single event had a maximum *F* of 111.7 during a 17.4 mm rainfall.

Tanaka et al. (1996) observed that in a red pine (*Pinus densiflora*) forest in Japan,stemflow inputs were concentrated over localized circular areas at the tree base, and showed strong vertical movement in the soil profile. They found that all stemflow infiltrates within a 50 cm radius around large trees (circumferences > 40 cm) and approximately 30 cm radius around smaller trees (circumferences < 20 cm). The amount of water concentrated was so large that it represented an important groundwater recharge mechanism in this pine forest. Vincke and Thiry (2008) have shown that water tables near the soil surface not only provided a key source of water for trees and other vegetation, but often show diurnal fluctuations. In the day when evapotranspiration is occurring, the water table declines, whereas at night the water table rebounds due to the absence of evapotranspiration. Furthermore, stemflow production by beech (*Fagus sylvatica*) was linked to the fast response portion of a storm hydrograph from a hillslope in eastern England (Crabtree and Trudgill, 1985).This has been shown to contribute vast amounts of concentrated nutrients at the base of trees creating 'fertile islands' (Whiteford *et al*., 1997). Thus, although a minor component of the forest water balance, stemflow, because of its concentrated demeanor, may be an important hydrologic mechanism for other components of the forest water cycle.

Macropores are one explanation of how stemflow precipitation can reach the water table. With macropore flow, soil water can flow faster and deeper by channeling infiltrated water along roots through preferential flow pathways that are formed by localized compaction of soil by roots. In the active rhizosphere along living roots and old root channels, these pathways influence water and nutrient distribution (Johnson and Lehmann, 2006). On forested hill slopes, localized concentrated stemflow inputs at the tree base bypassed the soil matrix through macropores leading to rapid inputs to a nearby stream (Levi and Frost, 2003). Li *et al*., (2009) have found that arid and semi-arid shrubs divert precipitation as stemflow where it infiltrates the soil and is stored in the deeper soil layers through stemflow-root channelization, for later when plant uptake is needed. This is thought to be an adaption to survive drought periods.

Canopy interception loss is when a proportion of rain falls is intercepted by the canopy and evaporates back into the atmosphere. Canopy interception loss , which often constitutes a ample portion of the total evaporation flux to the atmosphere from forests (Carlyle-Moses and Gash, 2011), is almost always derived by taking the difference between incident rainfall and the sum of TF and SF (e.g., Carlyle-Moses et al., 2010; Návar, 2013; Saito et al., 2013).

Throughout the world interception studies have been conducted in various climates and ecosystems producing interception results ranging from 10 to 50 % of annual or season-long rainfall (Roth et al. 2007). Canopy interception loss, *from* mature lodgepole pine forests or stands that comprise lodgepole pine with other species is appreciable, accounting for 24 – 29% of season-long rainfall (Spittlehouse, 1998; Moore et al., 2008). Interception is affected by numerous biological factors, including tree density, number of branches, species, height, basal area, crown projection area, and branch angel, as well as climatic factors such as intensity, amount and duration of rainfall. In addition wind speeds, direction, air temperature and humidity all effects interception pre and post event (Crockford and Richardson, 2000).

There have been several key models that have been developed for estimating Ic, ranging from analytical models such as the Gash model (Gash, 1979) to linear regression (Helvy and Patric, 1965), physical-based numerical (Rutter et al, 1971, 1975) and stochastic models (Calder, 1986).

Chapter 2 examines a juvenile lodgepole pine (*Pinus contorta* Douglas ex Louden var. *latifolia* Engelm. ex S. Watson) stand in south-central British Columbia, in order to determine the magnitude of point and structural *throughfall* as well as *stemflow* at the rainfall event and growing-season temporal scales. In addition, this chapter evaluates if *throughfall* (both point and structural) and *stemflow* spatial variability exhibits temporal persistence and if so attempt to determine what the influence, if any, tree and storm characteristics may have on this stability variability. Finally Chapter 2 provides recommendations for sampling strategies for future research in similar forested environments.

Chapter 3 deals with interception modelling based on original field observations conducted in the same previously mentioned lodgepole pine stand on the Bonaparte Plateau, north of Kamloops, British Columbia, Canada. The goal of this chapter was to evaluate the

performance of the reformulated Gash (Valente *et al*., 1997) and reformulated Liu (Carlyle-Moses and Price, 2007) I_c models at both event and season-long time scales, as well as to determine the quantitative importance of throughfall, stemflow and I_c. Furthermore, this chapter assesses if the data collected supports a 'water-box' or an 'exponential wetting approach' of the canopy saturation process.

REFERENCES

Axelson, J., Alfaro, R., Hawkes, B. 2009. Influence of fire and mountain pine beetle on the dynamics of lodgepole pine stands in British Columbia, Canada. *Forest Ecology and Management* **257**: 1874–1882.

B.C. Ministry of Forests, Mines and Lands. 2010. The State of British Columbia's Forests, 3rd ed. Forest Practices and Investment Branch, Victoria, B.C. www.for.gov.bc.ca/hfp/sof/index.htm#2010_report

Bellot, J., Escarre, A. 1998. Stemflow and throughfall determination in a resprouted Mediterranean holm-oak forest, *Annales des Sciences Forestieres* **55:** 847–865.

Brabender, B. 2005. Scaling leaf area index and Rainfall interception in Lodgepole pine. MSc Thesis, University of Alberta.

Calder, I.R. 1986. A stochastic model of rainfall interception. *Journal of Hydrology:* **89**: 65-71.

Carlyle-Moses DE, Park AD, Cameron JL. 2010. Modelling rainfall interception loss in forest restoration trials in Panama. *Ecohydrology* **3**: 272-283

Carlyle-Moses DE, Price AG. 2006. Growing-season stemflow production within a deciduous forest of southern Ontario. *Hydrological Processes* **20**: 3651-3663.

Carlyle-Moses DE, Price AG. 2007. Modelling canopy interception loss from a Madrean pine-oak stand, Northeastern Mexico. *Hydrological Processes* **21**: 2572-2580

Carlyle-Moses DE, Gash JHC. 2011. Rainfall Interception Loss by Forest Canopies. In: *Forest Hydrology and Biogeochemistry: Synthesis of Past Research and Future Directions*, Levia DF, Carlyle-Moses DE, Tanaka T (eds.). *Ecological Series* **216**, Springer-Verlag: Heidelberg, Germany; 407-423.

Carlyle-Moses DE, Flores Laureano J.S., Price A.G. 2004. Throughfall and throughfall spatial variability in Madrean oak forest communities of northeastern Mexico. *Journal of Hydrology* **297**:124-135.

Crabtree, A.F., Trudgill, S.T., 1985. Hillslope hydrochemistry and stream response on a wooded, permeable bedrock: the role of stemflow. *Journal of Hydrology* **80:** 161–178.

Crockford, R. H., Richardson, D. P.2000, Partitioning of rainfall into throughfall, stemflow and interception: effect of forest type, ground cover and climate. *Hydrological Processes* **14:** 2903–2920.

Gash JHC. 1979. An analytical model of rainfall interception in forests. *Quarterly Journal of the Royal Meteorological Society* **105**: 43-55

Gomez, J.A., Vanderlinden, K., Gira´ldez, J.V., Fereres, E., 2002. Rainfall concentration under olive trees. *Agricultural Water Management* **55**: 53–70.

Helvey, J. D., Patric J. H.1965. Canopy and litter interception of rainfall by hardwoods of eastern United States, *Water Resour. Res., 1(2)*

Herwitz SR. 1986. Infiltration-excess caused by Stemflow in a cyclone-prone tropical rainforest. *Earth Surface Processes and Landforms* **11:**401-412.

Holwerda F., Scatena F.N, Bruijnzeel L.A. 2006. Throughfall in a Puerto Rican lower montane rain forest: A comparison of sampling strategies. *Journal of Hydrology* **327**: 592-602.

Huber A., Iroumé A .2001. Variability of annual rainfall partitioning for different sites and forest covers in Chile. *Journal of Hydrology* **248**:78–92

Hupet F., Vanclooster, M., 2001. Effect of the sampling frequency of meteorological variables on the estimation of the reference evapotranspiration. *Journal of Hydrology* **243**: 192–204

Johnson MS., Lehmann J. 2006. Double-funnelling of trees: Stemflow and root-induced preferential flow. *Ecoscience* **13**: 324-333.

Keim, R.F., Skaugset, A.E., Weiler, M., 2005. Temporal persistence of spatial patterns in throughfall. *Journal of Hydrology* 314: 263–274.

Levia DF Jr., Frost EE. 2003. A review and evaluation of stemflow literature in the hydrologic and biogeochemical cycles of forest and agricultural ecosystems. *Journal of Hydrology* **274**: 1-29.

Li, X, Liu, L., Gao, S., Ma., Y., Yan, Z. 2008. Stemflow in three shrubs and its effect on soil water enhancement in semiarid loess region of China. *Agricultural and Forest Meteorology* **148**: 1501-1507.

Li X., Yang, Z., Lim Y, Lin H. 2009. Connecting ecohydrology and hydropedology in desert shrubs: stemflow as a source of preferential flow in soils. *Hydrology and Earth System Science* **13:** 113-1144.

Loescher, H.W., Powers, J.S., Oberbauer, S.F., 2002. Spatial variation of throughfall volume in an old-growth tropical wet forest, Costa Rica. *Journal of Tropical Ecology* **18:** 397–407

Lousteau, D., Berbigier, P., Granier, A. 1992. Interception loss, throughfall and stemflow in a maritime pine stand, II. An application of Gash's analytical model of interception. *Journal of Hydrology* **138**: 469–485.

McKee AJ 2010. The quantitative importance of stemflow: An evaluation of past research and
results from a study in lodgepole pine (Pinus contorata var. latifolia) stands in southern British Columbia. M.Sc. in Environmental Science thesis, Thompson Rivers University.

McKee AJ., Carlyle-Moses DE. 2010. Stemflow: A potentially important point source of water for growth. *Linking Innovations and Networking Knowledge* **11**:11-12.

Moore, RD, Winkler, RD, Carlyle-Moses, DE (2008) Watershed response to the McLure forest fire: presentation summaries from the Fishtrap Creek workshop, March 2008. *Streamline Watershed Manage Bulletin* **12**: 1-11

Nadkarni N., and Sumera M. 2004. Old-Growth Forest Canopy Structure and Its Relationship to Throughfall Interception. Forest Science **50**: 290-298

Návar J. 2013. The performance of the reformulated Gash's interception loss model in Mexico's northeastern temperate forests. *Hydrological Processes* **27**: 1623-1633

Navar, J., Bryan, R.B., 1990. Interception loss and rainfall redistribution by three semi-arid growing shrubs in northeastern Mexico. *Journal of Hydrology* **115**: 51–63

Price A.G., Dunham K, Carleton T. 1997. Variability of water fluxes through the black spruce (Picea mariana) canopy and feather moss (Pleurozium schreberi) carpet in the boreal forest of northern Manitoba. *Journal of Hydrology* **196**:310–323

Roth, BE, Slatton, KC, Cohen, MJ. 2007. On the potential for high-resolution lidar to improve rainfall interception estimates in forest ecosystems. *Frontiers in Ecology and the Environment* **5**: 421-428

Rutter, AJ, Kershaw, KA, Robins, PC. 1971. A predictive model of rainfall interception in forests I: derivation of the model from observations in a plantation of Corsican pine. *Agricultural Meteorology* **9**: 367-384

Rutter, A., Morton, A., Robin, P., 1975. A Predictive Model of Rainfall Interception in Forests. II. Generalization of the Model and Comparison with Observations in Some Coniferous and Hardwood Stands. *Journal of Applied Ecology* **12**: 367–380

Saito T, Matsuda H, Komatsu M, Xiang Y, Takahashi A, Shinohara Y, Otsuki K. 2013. Forest canopy interception loss exceeds wet canopy evaporation in Japanese cypress (Hinoki) and Japanese cedar (Sugi) plantations. *Journal of Hydrology* **507**: 287-298

Spittlehouse, DL 1998. "Rainfall Interception in Young and Mature Coastal Conifer Forests." In: *Mountains to Sea: Human Interaction with the Hydrological Cycle, Y. A1i1a (ed.),* Canadian Water Resources Association, Cambridge.

Staelens J, Schrijver AD, Verheyen K, Verhoest N. 2006. Spatial variability and temporal stability of throughfall water under a dominant beech (Fagus sylvatica L.) tree in relationship to canopy cover. *Journal of Hydrology* **330**: 651-662

Taniguchi M, Tsujimura M, Tanaka T. 1996. Significance of stemflow in groundwater recharge. 1: Evaluation of this stemflow contribution to recharge using a mass balance approach. *Hydrological Processes* **10**: 71-80

Tanaka T, Taniguchi M, Tsujimura M. 1996. Significance of stemflow in groundwater recharge. 2: A cylindrical infiltration model for evaluating the stemflow contribution to groundwater recharge. *Hydrological Processes* **10**:81-88

Valente, F., David, J.S., Gash, J.H.C., 1997. Modelling interception loss for two sparse eucalypt and pine forests in central Portugal using reformulated Rutter and Gash analytical models. *Journal of Hydrology* **190**: 141–162

Van Stan II JT, Stiegert CM, Levia DF, Scheick CE. 2011. Effects of wind-driven rainfall on stemflow generation between codominant tree species with differing crown characteristics. *Agricultural and Forest Meteorology* **151**:1277-1286

Vincke C, Thiry Y. 2008. Water table is a relevant source for water uptake by a Scots pine (Pinus sylvestris L.) stand: Evidences from continuous evapotranspiration and water table monitoring. *Agricultural and Forest Meteorology* **148**: 1419–1432

Whitford WH, Anderson J, Rice PM. 1997. Stemflow contribution to the 'fertile island' effect in creosote bush, *Larrea tridentate*. *Journal of Arid Environments* **35**: 451-457

CHAPTER 2
THROUGHFALL HETEROGENEITY AND TEMPORAL PERSISTENCE BELOW AND BETWEEN THE CANOPIES OF JUVENILE LODGEPOLE PINE (*Pinus contorta*)

INTRODUCTION

Rain falling on a forest is either stored on the canopy and subsequently evaporates (canopy interception loss) or it is routed by the canopy into understory precipitation. Understory precipitation takes two forms - throughfall, *TF*, which reaches the forest floor by passing through canopy gaps or by dripping from vegetation components, and stemflow, *SF*, which reaches the ground by flowing down tree boles. At the plot-scale and beyond, *TF* represents the largest volumetric component of understory precipitation, often accounting for > 70% of gross precipitation at season-long or annual time scales (Carlyle-Moses and Price, 2007; Levia *et al*., 2011; Macinnis-Ng *et al*., 2012), while *SF* is usually volumetrically minor at this spatial scale, commonly representing < 5% of seasonal or gross precipitation (e.g., Helvey and Patric, 1965; Marin *et al*., 2000; Reid and Lewis, 2009). Thus, *TF* represents a relatively large component of understory precipitation and the quantity of water available for the terrestrial portion of the hydrologic cycle. Throughfall is also a key transfer mechanism in the biogeochemical cycles of wooded ecosystems (Parker, 1983; Levia *et al*., 2011; Bhat *et al*., 2011).

Canopy interception loss - which often constitutes a sizable portion of the total evaporation flux to the atmosphere from forests (Carlyle-Moses and Gash, 2011) - is almost always derived by taking the difference between incident rainfall and the sum of *TF* and *SF* (e.g., Carlyle-Moses *et al*., 2010; Návar, 2013; Saito *et al*., 2013). Given the quantitative importance of *TF* compared to *SF* at the spatial scales in which canopy interception loss estimates are made, *TF* spatial variability is an important consideration since any errors accompanying estimates of the mean areal *TF* will be propagated in the canopy interception loss estimate. Thus, accurate estimates of *TF* magnitudes are a requisite for hydrological and biogeochemical studies conducted in forests; however, obtaining this accuracy poses a methodological challenge (Lloyd and Marques, 1988; Holwerda *et al*., 2006; Zimmermann and Zimmermann, 2014), largely due to the spatial heterogeneity of this hydrologic input (e.g., Loustau *et al*., 1992; Price *et al*., 1997; Marin *et al*., 2000; Price and Carlyle-Moses, 2003).

Although much is yet to be learned (see Pypker *et al*., 2011), spatially varying *TF* inputs have been attributed to the complexity of the forest cover including overlapping tree canopies, varying tree heights, canopy gaps, and the arrangement and variation in leaf and branch area (Zirlewagen and von Wilpert, 2001; Carlyle-Moses *et al*., 2004; Konishi *et al*., 2006; Staelens *et al*., 2006; Poppenborg and Hölscher, 2009; Nanko *et al*., 2011). Additionally, *TF* heterogeneity may be dependent on meteorological factors such as rainfall depth and intensity, as well as wind speed and direction (e.g., Herwitz and Slye, 1995; Carlyle-Moses 2004; David *et al*., 2006; Zimmermann *et al*., 2008). In some forests the interaction of rainfall with the canopy produces systematic *TF* spatial patterns, such as where *TF* varies as a function of the distance from the tree bole (e.g., Stout and McMahon, 1961; Ford and Deans, 1978; Pedersen, 1992). In other forests, presumably due to the intricacy in canopy composition, patterns of *TF* may be considered spatially random (Loustau *et al*., 1992; Carlyle-Moses *et al*., 2004). Much focus has been paid to the spatial heterogeneity of *TF*, especially as it influences *TF* sampling in terms of the number of individual gauges used to meet certain statistical objectives related to the *TF* estimate (e.g., Kimmins, 1973; Puckett, 1991; Price and Carlyle-Moses, 2003), the periodic reassignment of gauge locations (e.g., Lloyd and Marques, 1988; Ziegler *et al*. 2009; Ritter and Regalado, 2014), and the type of gauge used (Zimmermann *et al*., 2010; Carlyle-Moses *et al*., 2014).

Although an important consideration for *TF* sampling, *TF* heterogeneity may also represent a connection between canopy structure and ecosystem functioning at the understory level and within the soil profile (Ford and Deans, 1987; Carleton and Kavanagh, 1990; Bouten *et al*., 1992; Manderscheid and Matzner, 1995). If such linkages exist in a particular forest, the potential importance of *TF* spatial patterns on these various ecohydrologic processes would either necessitate or at least be more pronounced if the spatial delivery of *TF* was stable over time (Keim *et al*., 2005). The temporal persistence of *TF* spatial input has been studied in tropical (Zimmermann *et al*., 2007; Zimmermann *et al*., 2008; Wullaert *et al*., 2009), temperate deciduous (e.g., Keim *et al*., 2005; Gerrits *et al*., 2010) and temperate coniferous forests (e.g., Raat *et al*., 2002; Keim *et al*., 2005; Carlyle-Moses *et al*., 2014), as well as within a eucalyptus plantation (Sato *et al*. 2011). Additionally, the temporal stability of *TF* spatial variability has been examined at the tree-scale for two deciduous species (see Staelens *et al*., 2006; Fathizadeh *et al*., 2014). Temporally stable patterns in *TF* delivery

observed in these studies ranged from relatively 'weak' (e.g., Gerrits *et al*., 2010) to 'significant' (e.g., Staelens *et al*., 2006), suggesting that linkages, if any do exist, between the spatial variability of *TF* and ecohydrological processes at the understory or within the soil may be forest or tree-type dependent.

Mountain pine beetle (*Dendroctonus ponderosae* Hopkins) (MPB) has severely affected the majority of pine species in the province of British Columbia, Canada, especially lodgepole pine (*Pinus contorta* Douglas ex Louden var. *latifolia* Engelm. ex S. Watson). By 2004, more than seven million hectares of lodgepole pine forests were infested by MPB in the province (Rice *et al*., 2007). The loss of mature lodgepole pine stands, including those lost to salvage logging, has resulted in larger portions of the province being covered by juvenile pine stands through planting and natural regrowth. With this change from mature to juvenile cover at such a large scale, questions regarding the hydrology and ecosystem functioning of impacted areas have been raised (Uunilla *et al*., 2006). Studies evaluating canopy water balance dynamics in mature and juvenile lodgepole pine stands have found that young stands produce volumetrically greater *TF* and *SF* than their mature counterparts (e.g., Spittlehouse, 1998); however, no studies to date have examined of the spatiotemporal patterns associated with this increased *TF* in juvenile lodgepole pine environments. Such studies are a requisite to improving our understanding of the hydro-ecological impacts of disturbance regimes, such as MPB, in these and similar environments.

The objectives of this study, are to: i) determine the magnitude and spatial variability, expressed by the coefficient of variation *CV*, of *TF* under four structurally distinct areas of canopy coverage (inner-canopy, mid-canopy, canopy-periphery, and areas free of cover between individual canopies [outside-of-canopy]), ii) evaluate if *TF* spatial variability exhibits temporal persistence and if so to determine what the influence, if any, certain tree and storm characteristics have on this stability, and iii) based on meeting objectives i and ii, to provide recommendations for sampling strategies and for future research in these and similar forests.

MATERIALS AND METHODS

Study area

Measurements of rainfall and *TF* were conducted at the Mayson Lake hydrological research area, which is located on the Thompson-Bonaparte plateau approximately 60 km NNW of Kamloops, British Columbia, Canada (51°12'49" N 120°23'43" W) at an elevation of 1290 m a.m.s.l. (Figure 2.1).

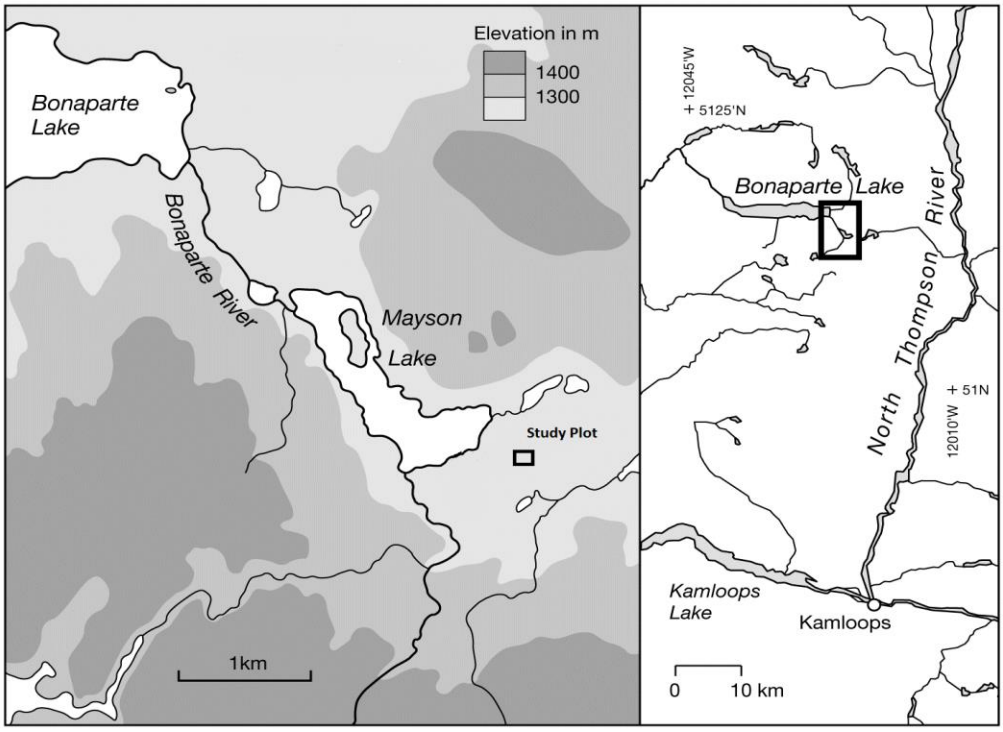

Figure 2.1: Geographic Location of the study plot. Adapted from Winkler *et al*. (2010).

The study area has a long-term (1981-2010) mean annual precipitation depth of ~ 640 mm with ~280 mm falling during the growing-season (mid-May through early October) (Wang *et al*., 2006; 2012). Precipitation in the form of rainfall dominates the growing-season period, while precipitation during the dormant season is largely comprised of snow. Mean annual temperature is 3.3 ^{o}C, with mean monthly temperatures ranging from -7.1 ^{o}C in December to 13.9 ^{o}C in July. The Köppen climate classification for the region is Dfc (sub-arctic) while the provincial Biogeoclimatic Ecosystem Classification designation (BC Ministry of Forests and Range, 2008) is Montane Spruce dry mild variant (B.C. Ministry of Forests and Range, 2008).

The plot selected for this study was harvested in 1999 and planted with lodgepole pine seedlings within the following 2 years. Point-centered quarter analysis (Cottam and Curtis, 1956) revealed that in 2010 the plot (2600 m^2) was dominated by lodgepole pine with 5640 stems ha^{-1}, and a basal area of 9.6 m^2 ha^{-1}, while subalpine fir represented 980 stems ha^{-1}, and a basal area of 0.6 m^2 ha^{-1}. No other tree species occurred in the plot. Average lodgepole pine tree height was ~ 2.2 m (median ~1.7 m), with a maximum height of 5.2 m. Average projected crown area (PCA) of the pines was ~ 0.9 m^2 (median ~ 0.5 m^2), with a maximum of 3.2 m^2, while the total PCA of the plot was ~ 4940 m^2 ha^{-1}. Although trees sometimes occurred in groups with overlapping crowns, the majority of crowns, including those of the trees in which *TF* was sampled, occurred in isolation from one another.

Rainfall and throughfall measurement

Rainfall depth and intensity were measured on an event basis from May 16 – October 4, 2010 using an Onset® tipping bucket rain gauge (model # S-RGB-M002) with a diameter of 15.4 cm, resolution = 0.2 mm tip^{-1}. Additionally, rainfall depth was measured with a Meteorological Service of Canada Type-B rain gauge (diameter = 11.3 cm). The tipping bucket and the Type-B gauge openings were situated 1 m above the ground surface, located ~ 40 m south-west of the site. A rain event was defined as a period of rainfall bounded by 8 hours with no measurable rainfall as indicted by the tipping bucket rain gauge record in conjunction with Canada's National Climate Data and Information Archive 10-minute time step radar imagery (Silver Star Mountain Doppler radar station). An 8 hour bound for individual events was selected as this was the time required for canopies in this and a similar plot in the area to completely dry (McKee, 2010). Weather radar was also used to determine the number and duration of intra-storm breaks ≥ 10 minutes and the direction of storm origin. Wind speed and direction data were collected using an Onset® weather station (Hobo® Micro Station Data Logger – H21-002 and associated sensors). However, the data files associated with this station were corrupted and as such the data were not available for analysis.

Throughfall was measured on an event basis under the isolated crowns of nine trees, the characteristics of which are provided in Table 2.1. For each tree 16 manually-read Tru-Chek® wedge gauges (catch area = 36.3 cm^2 each) were used, with four of these gauges placed along four transects (N, W, S, E). Along each transect one gauge was placed adjacent

Table 2.1: Characteristics of the individual lodgepole pine trees used in this study. Correlations among the tree size metrics were all significant ($p \leq 0.05$): Height – Basal Area ($r = 0.908$; $r_s = 0.933$); Height – Projected Crown Area ($r = 0.909$; $r_s = 0.933$), Basal Area – Projected Crown Area ($r = 0.999$, $r_s = 1.0$).

Tree ID	Height (m)	Basal Area (cm^2)	Projected Crown Area (m^2)
1	1.39	6.5	0.48
2	1.88	14.5	0.78
3	1.20	3.6	0.38
4	2.68	18.4	0.93
5	3.00	37.1	1.62
6	2.14	13.2	0.74
7	3.69	28.4	1.30
8	3.22	40.6	1.75
9	4.22	66.5	2.71

to the tree bole (inner-canopy), one at the mid-canopy point, one at the canopy-periphery, and the fourth gauge situated at a random distance in the open area between tree canopies, but within 45˚ of the top of the selected tree.

Canopy cover

Canopy cover fraction was determined above each *TF* gauge under the three below-canopy zones using methods similar to those Staelens *et al*. (2006). Digital non-hemispherical colour photographs (Canon Powershot A40) were taken vertically (using a bull's-eye spirit level) at the height of the top of each gauge (Llorens and Gallart, 2000; Staelens *et al*., 2006) under overcast conditions in early October 2010. Photographs were scaled to an equivalent size of the *TF* gauge opening (approximately 36 cm^2) centered on the first branching level from the ground. Canopy cover fraction was then derived using Geomatica 10.3.2. (PCI Geomatics Inc., Richmond Hill, Ontario) using supervised pixel classification of the scaled photograph. Because of the overlap between needle and wood components in the canopy, no attempt was made to determine the fraction of the canopy that was foliage and that which was wood.

Temporal persistence of throughfall

Temporal persistence has been analyzed using differing techniques, many of which assume that the distribution of the variable of interest follows a normal distribution (e.g., Vachaud *et al*., 1985; Raat *et al*., 2002; Keim *et al*., 2005). However, at the rainfall event scale *TF* often does not exhibit a normal distribution (e.g., Lloyd and Marques, 1988; Loustau *et al*., 1992)

and thus the method of standardizing *TF* used by Zimmermann *et al*. (2008), in which each stationary *TF* gauge is corrected to zero median and unit variance, was used in this study:

$$TFS_i = \frac{TF_i - TF_{median}}{MAD} \quad (2.1)$$

where, TFS_i is the standardized value of the throughfall depth measured for an individual gauge, TF_i (mm), TF_{median} is the median *TF* depth (mm) of all gauges, and *MAD* represents the median absolute deviation of *TF*(mm).

A plot of TFS_i for each event and for each *TF* gauge, ranked from minimum to maximum mean TFS_i, shows the deviation of TFS_i for all *TF* sampling points (Zimmerman *et al*., 2008). These temporal stability plots show two types of persistence – *extreme* persistence, referring to mean TFS_i values that deviate from the median and are within either the upper or lower quartiles of the mean TFS_i ranked gauges, and *general* persistence, which refers to the TFS_i that deviate from the median TFS_i and are within the interquartile range (Keim *et al*., 2005; Zimmermann *et al*., 2008). Although others have used ± 1 standard deviation as a criterion for persistence (e.g., Raat *et al*., 2002; Wullaert *et al*., 2009), Zimmermann *et al*. (2008) suggest the stricter criterion of using the 95% confidence limits of the mean TFS_i. For comparative purposes with previous studies both the ± one standard deviation and the 95% confidence limits of the mean TFS_i are used in this study. Additionally, mean TFS_i values were examined to determine if they were significantly different than zero at the 95% confidence level (Carlyle-Moses *et al*., 2014), which would indicate non-random spatial patterns over time even if they did not meet the established criteria for persistence.

Following Zimmermann *et al*. (2008), Spearman rank correlation coefficients, r_s, for all possible event pairings (n = 703) for *TF* were derived and examined to determine whether r_s could be modeled as a function of the temporal lag (days) between rainfall events, Δday. If r_s is a function of Δday then a change to the spatial pattern of *TF* through time can be identified. Similar to Zimmermann (2008), differences in storm characteristics (rainfall depth ΔP, event duration ΔD_E, rain duration ΔD_R, mean rainfall intensity ΔI_{Mean}, maximum 30 minute rainfall intensity $\Delta I_{Max\text{-}30}$, the number of intra-storm breaks ≥ 1 h each ΔN_B and their duration ΔD_B, and the direction of storm origin $\Delta DoSO$ were included as additional variables

to determine what influence, if any, they may have on variations in r_s. The best model was then selected using the Akaike information criterion (Sakamoto *et al*., 1986) in keeping with Zimmermann *et al*. (2008). The above procedure was conducted on all *TF* data from all four sampling zones pooled and for each of the four sampling zones separately.

Data analysis

Statistical analysis was conducted using IBM® SPSS® Statistics Version 22 and Microsoft ® Excel 2010. Where means could not be compared – determined using the Shapiro-Wilk test (Shapiro and Wilk, 1965) for normality – analysis of differences were carried out using a Tukey-type median test (Mood, 1950; Levy, 1979; see Zar 1984) for multiple comparisons among medians or the Mann-Whitney test (Mann and Whitney, 1947) when two medians were compared.

RESULTS

Incident precipitation

A total of 41 precipitation events ≥ 0.4 mm occurred during the course of this study. Two of these events fell as a mix of rain and snow, while one rainfall event was not collected as instrumentation was temporally removed due to a wildfire in close proximity to the site. For the remaining 38 events, total rainfall depth was 252.9 mm, or approximately 90% of the mean growing-season rainfall for the site. Individual rain events ranged from 0.5 mm (Event 7) to 30.8 mm (Event 4). Meteorological characteristics of each of these events along with the date of event occurrence are provided in Table 2.2. The direction of storm origin was predominately westerly with 30 of the events (79%) having a storm origin ranging from SSW to NNW, with 19 of these events (50% of all events) having a south-westerly (SSW – WSW) origin. Five events (13%) had a south-easterly origin (SSE – ESE), while only 2 events (5%) came from a north-easterly direction. One event (Event 1) came directly from the south.

Absolute and relative throughfall depth

Data were available for 5459 (99.8%) of the possible 5472 point *TF* measurements (144 *TF* gauges x 38 rain events), with the remainder discarded due to the gauges being disturbed before

Table 2.2: Event number, date(s) of occurrence, rainfall depth (P, mm), event duration (D_E, h), rainfall duration (D_R, h), mean rainfall intensity(I_{Mean}, mm h^{-1}), maximum 30 minute rainfall intensity, $I_{Max\text{-}30}$, mm h^{-1}), number of intra-storm breaks ≥ 1 h, (N_B), total duration of intra-storm breaks ≥ 1 h (D_B, h) and the principal cardinal direction of storm origin (*DoSO*).

Event #	Event Date (2010)	P (mm)	D_E (h)	D_R (h)	I_{Mean} (mm h^{-1})	$I_{Max\text{-}30}$ (mm h^{-1})	N_B	D_B (h)	*DoSO*
1	05 / 17	5.9	4.8	4.8	1.2	3.1	0	0.0	S
2	05 / 18	1.5	5.5	4.8	0.3	0.4	0	0.0	SW
3	05 / 26	0.7	4.2	3.3	0.2	0.2	0	0.0	SSE
4	05 / 27 - 30	30.8	72.0	29.3	1.1	5.0	13	32.5	SE
5	05 / 31 - 06 / 03	16.8	63.0	19.0	0.9	9.6	11	36.3	SW
6	06 / 04 - 05	7.5	19.7	14.0	0.5	0.8	2	2.7	SSW
7	06 / 05	0.5	3.3	2.7	0.2	0.5	0	0.0	SSW
8	06 / 07	0.8	3.2	1.0	0.8	0.3	1	1.2	WSW
9	06 / 07 - 08	9.1	24.3	8.2	1.1	11.5	4	15.0	WSW
10	06 / 08 - 11	20.5	65.0	33.3	0.6	1.8	11	26.2	SSE
11	06 / 15	20.0	8.2	6.3	3.2	8.8	1	1.5	NE
12	06 / 21	7.0	2.8	2.8	2.5	9.5	0	0.0	SW
13	06 / 22	2.5	7.7	3.2	0.8	4.1	1	4.0	SW
14	06 / 25	6.7	26.2	6.7	1.0	5.7	3	14.7	SW
15	06 / 30	1.3	3.3	1.7	0.8	0.8	1	1.2	WSW
16	07 / 04	12.8	17.2	8.7	1.5	3.8	3	7.0	NW
17	07 / 12	6.2	11.5	4.2	1.5	5.4	4	5.2	WNW
18	07 / 13	5.0	3.3	3.3	1.5	2.7	0	0.0	NNE
19	07 / 20	2.4	6.7	2.2	1.1	3.2	3	4.0	NNW
20	07 / 21 - 22	2.1	25.2	4.5	0.5	2.3	5	19.5	WNW
21	08 / 03	1.4	0.7	0.7	2.1	2.1	0	0.0	NW
22	08 / 07 - 08	8.0	29.0	3.3	2.2	5.4	5	24.3	W
23	08 / 08 - 09	5.9	30.8	11.0	0.5	1.8	7	18.7	WSW
24	08 / 21 - 22	6.0	23.3	4.2	1.4	3.6	3	19.2	SW
25	08 / 26 - 27	16.4	21.8	6.5	2.5	9.9	7	15.3	SW
26	08 / 29	1.4	0.5	0.5	2.8	2.8	0	0.0	WNW
27	08 / 31 - 09 / 01	6.4	28.0	13.3	0.5	3.6	4	14.7	WSW
28	09 / 04	5.7	1.0	1.0	5.7	7.7	0	0.0	SW
29	09 / 06 - 07	15.1	23.7	15.2	1.0	1.1	3	6.5	WNW
30	09 / 07 - 08	4.9	1.7	1.7	2.9	6.6	0	0.0	SE
31	09 / 08	1.7	3.5	2.2	0.8	1.4	1	1.3	ESE
32	09 / 10 - 11	6.8	6.0	6.0	1.1	2.7	0	0.0	W
33	09 / 15 - 16	2.4	10.2	5.0	0.5	1.4	3	4.0	NW
34	09 / 23 - 24	1.9	2.2	1.8	1.0	1.4	0	0.0	SW
35	09 / 24	3.2	2.2	2.2	1.5	2.7	0	0.0	SW
36	09 / 26	0.7	2.3	1.5	0.5	0.6	0	0.0	SW
37	09 / 28	2.3	3.7	1.8	1.3	2.7	1	1.5	WNW
38	10 / 10	2.6	2.2	1.0	2.6	3.0	0	0.0	SW

a measurement could take place. Throughfall data were collected for all 38 events from 132 of the 144 (91.7%) sample points. When all gauges are considered, cumulative point *TF* depths ranged from 69.1 mm (27.3% of rainfall) for the gauge situated in the inner-canopy zone of Tree 7 along the north transect to 327.9 mm (129.7% of rainfall) for the gauge located at the canopy-periphery of the southern transect of Tree 8. Thus, over the study

period cumulative point *TF* was found to range by 258.8 mm, slightly greater than the cumulative rainfall depth, and had a maximum cumulative *TF* to minimum cumulative *TF* ratio of 4.7. At the rainfall event scale the relative *TF* ranges were often much greater. For example, during Event 2 with a rainfall depth of 1.5 mm, *TF* was found to range from 0.0 mm for two gauges (along the east transect of Tree 8 in the inner-canopy and mid-canopy zones) to 6.4 mm (426.7% of rainfall) in the canopy-periphery zone along the south transect of Tree 4.

For comparative purposes with other studies (e.g., Staelens *et al*., 2006; Fathizadeh *et al*., 2014) and given the range and frequency of rain event depths, cumulative *TF* was derived for four rain depth classes: < 2 (n = 10), 2 to < 5 (n = 8), 5 to < 10 (n = 13), and ≥ 10 mm (n = 7). Additionally, for meaningful comparisons among the different rain depth classes *TF* was expressed as a percentage of cumulative rainfall, *TF*% (Sato *et al*., 2011; Fathizadeh *et al*., 2014). There was a tendency for *TF*% to increase with both increasing distance from the tree bole and with increasing size of the rainfall depth class (Figure 2.2). The *TF*% frequency distributions of the inner-canopy zone for the 5 to < 10 mm, and ≥ 10 mm rain depth classes as well as for the entire season significantly differed from the normal distribution, as did the cumulative *TF*% distributions associated with < 2, 5 to < 10 mm, and ≥ 10 mm rain depth classes for the canopy-periphery zone (Shapiro –Wilk test, $p \leq 0.05$). The median cumulative *TF*% values for the four rain depth classes and for the season significantly differed ($p \leq 0.05$) among the sampling zones. The exceptions were i) cumulative median *TF*% for the inner-canopy and mid-canopy zones did not significantly differ for the < 2 and 2 to < 5 mm rain depth classes, and ii) mid-canopy zone and canopy-periphery zone cumulative *TF*% were not significantly different ($p \leq 0.05$) under the ≥ 10 mm rain depth class and for the cumulative season rainfall scenario.

Throughfall spatial variability

Figure 2.3a shows that the spatial variability of accumulated *TF* depth (mm), expressed by the coefficient of variation (*TF CV*%), decreased in an asymptotic fashion with accumulated rainfall depth for all four sampling zones. Once the first five rain events of the study (totaling 55.7 mm) had fallen, *TF CV*% remained stable at approximately 30, 26, and 18% for the

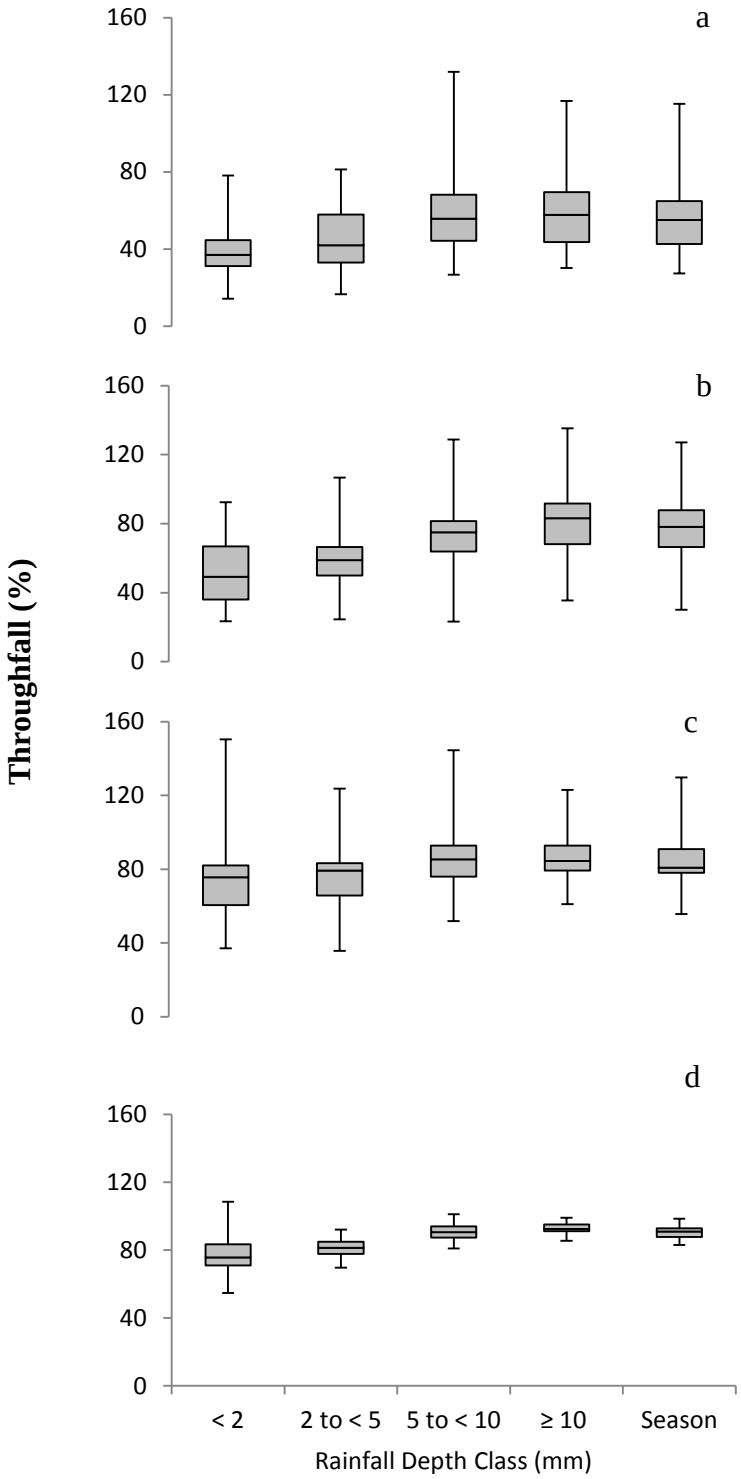

Figure 2.2: Box-plots of cumulative *TF*% for different rain depth classes and for the season for the different sampling zones: a) inner-canopy, b) mid-canopy, c) canopy-periphery, and d) outside-of-canopy.

inner-canopy, mid-canopy, and canopy-periphery zones, respectively. Accumulated *TF CV*% for gauges situated in the outside-of-canopy zone reached a stable value of approximately 4% once four events with an accumulated rainfall depth of 38.9 mm had fallen. At the rainfall event scale, *TF CV*% decreased asymptotically with increasing rainfall depth for all sampling zones, including the outside-of-canopy zone (Figure 2.3b).

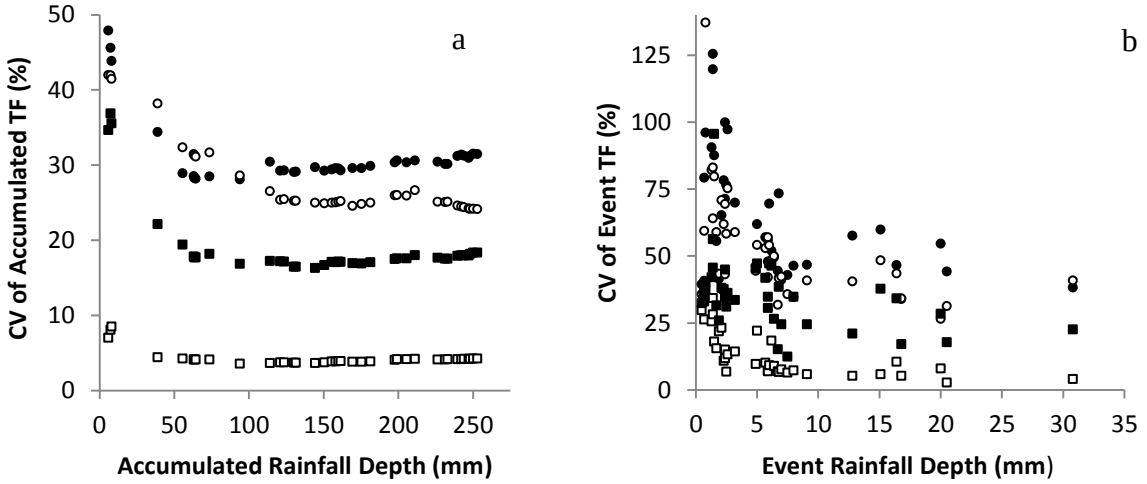

Figure 2.3: Accumulated (a) and event (b) TF CV% as a function of rain depth for the inner-canopy (closed circles), mid-canopy (open circles), canopy-periphery (closed squares) and outside-of-canopy (open squares).

Using the Shapiro-Wilk test the frequency distributions of *TF CV*% for all sampling zones were found to be significantly different ($p \leq 0.05$) than the normal distribution. As with cumulative *TF*%, differences among and between median *TF CV*% values of the different sampling zones were assessed using nonparametric tests. The median value of *TF CV*% for gauges situated in the outside-of-canopy zone (10.3%) was significantly lower (Mann-Whitney test, $p < 0.001$) than that of gauges under the canopy, i.e., all three below-canopy zones combined, (50.2%). When the three below-canopy zones are compared significant differences ($p \leq 0.05$) were found between median *TF CV* % values between the inner-canopy gauges (56.4%) and those situated at the canopy-periphery (34.6%) and between gauges located within the mid-canopy zone (48.4%) and those at the canopy-periphery. No significant difference ($p \geq 0.05$) was found between the median *TF CV*% of the inner-canopy zone and the mid-canopy zone. Significant r_s values ($p \leq 0.05$) between

event *TF CV*% for each sampling zone and various rain event characteristics are provided in Table 2.3.

Table 2.3: Spearman rank correlation coefficients (n = 38) between the *CV* of event *TF*% and the storm characteristics of rainfall depth, P (mm), event duration, D_E (h), mean rainfall intensity I_{Mean} (mm h^{-1}), maximum 30-minute rainfall intensity, $I_{Max\text{-}30}$ (mm h^{-1}), number of storm breaks ≥ 30 minutes, N_B, and total duration of those breaks, D_B (h). Level of significance: $^{*}p \leq 0.05$; $^{**}p \leq 0.01$.

TF CV%	P (mm)	D_E (h)	I_{Mean} (mm h^{-1})	$I_{Max\text{-}30}$ (mm h^{-1})	N_B	D_B (h)
Inner-Canopy	-0.488**	-0.372*	0.059	-0.335*	-0.299	-0.300
Mid-Canopy	-0.649**	-0.467**	-0.019	-0.369*	-0.305	-0.333*
Canopy-Periphery	-0.491**	-0.465**	0.212	-0.239	-0.393*	-0.404*
Outside-of-Canopy	-0.871**	-0.661**	-0.114	-0.515**	-0.524**	-0.571**

Throughfall, tree size and canopy cover

No significant Spearman or Pearson correlations ($p \leq 0.05$) were found among tree size metrics (tree height, basal area, and projected canopy area) and the median of cumulative *TF*% for any rain depth class or for cumulative rain over the season for both the inner-canopy and outside-of-canopy zones. However, tree size characteristics were found to be correlated with median cumulative *TF*% in the mid-canopy zone for smaller rain depth classes and with canopy-periphery median *TF*% for the largest rain depth class (≥ 10 mm) and cumulative season rainfall (Table 2.4).

Cumulative season-long *TF*% was found to be significantly correlated ($p \leq 0.01$) with canopy cover fraction (%) above the gauge when all three below-canopy sampling zones are grouped together (r_s = -0.517, r = -.459, n = 99). However, when cumulative *TF*% was compared with canopy cover fraction within each of the below-canopy zones separately, cumulative *TF*% was found to be only significantly correlated with canopy cover fraction for the < 2 mm ($p \leq 0.01$, r_s = -0.430, r = -0.465, n = 36) and 2 to < 5 mm rain depth classes ($p \leq 0.05$, r_s = -0.386, r = -0.360, n = 35) for the mid-canopy zone.

Throughfall and transect direction

Significant differences among median cumulative *TF*% values for different transect

Table 2.4: Spearman rank correlation coefficients ($n = 9$) between tree size characteristics and median cumulative *TF*% in each of the four sampling zones for four rain depth classes and for the entire season. Level of significance: $^{*}p \leq 0.05$, $^{**}p \leq 0.01$. Note: Basal area and PCA are listed together since the ranks of each of the tree basal areas of the nine trees match the ranks of each of the PCA values (i.e., $r_s = 1.0$).

Median Cumulative *TF*%	Rain Depth Class				
	< 2 mm	2 to < 5 mm	5 to < 10 mm	≥ 10 mm	Season
Inner-Canopy					
Tree Height	0.185	-0.150	-0.033	-0.367	-0.300
Basal Area or PCA	0.277	-0.167	0.033	-0.400	-0.300
Mid-Canopy					
Tree Height	-0.695**	-0.800**	-0.117	-0.500	-0.550
Basal Area or PCA	-0.628	-0.750*	-0.050	-0.533	-0.567
Canopy-Periphery					
Tree Height	0.267	0.167	-0.517	-0.833**	-0.767*
Basal Area or PCA	0.400	0.050	-0.417	-0.867**	-0.717*
Outside-of-Canopy					
Tree Height	0.467	0.008	0.000	-0.400	0.317
Basal Area or PCA	0.400	-0.042	0.232	-0.100	-0.233

directions under differing rain-depth classes and canopy zones were found (Table 2.5). These differences were largely limited to the inner-canopy and mid-canopy zones and for rain-depth classes at or below 5 to < 10 mm. However, the cumulative median *TF*% values of the south transect canopy-periphery and the east transect canopy-periphery also differed significantly, albeit at the $p \leq 0.10$ level. A trend is evident, and significant differences exist, in cumulative median *TF*% for east transects being lower than south and or west transects and, although less prevalent, north transect values being lower than those associated with west transects.

The influence of the direction of storm origin *DoSO*, on differences in *TF* between transects was evaluated by taking the ratio of the storm-ward *TF* to lee-ward *TF*. Storm-ward *TF* was equated with the median *TF* of a given canopy zone along the transect of the same direction when the *DoSO* was a cardinal direction (e.g., S), or, in the case where the *DoSO* was an intercardinal (e.g., SW) or a secondary-intercardinal direction (e.g., SSW) the median *TF* value was derived, respectively, as the average or the weighted average of the median *TF* of the two corresponding transects. The lee-ward *TF* was derived as above, but for the opposite cardinal, intercardinal, or secondary-intercardinal direction as the *DoSO*. Storm-

Table 2.5: Median cumulative *TF*% as a function of canopy position and transect direction (n = 9 for each case). Values in bold indicate medians that significantly differ (median test: $^{*}p \leq 0.10$, $^{**}p \leq 0.05$, $^{***}p \leq 0.01$) from one another with the transect direction of the differing value superscripted (N = north, S = South, E = east, and W = west).

Median Cumulative *TF*%	Rain Depth Class				
Position	< 2 mm	2 to < 5 mm	5 to < 10 mm	≥ 10 mm	Season
Inner-Canopy					
North	28.6	33.3	49.2	53.2	47.5
South	29.4	**37.5**^{E*}	**56.0**^{E*}	58.5	44.8
East	**25.0**^{W*}	**22.9**^{S*}	**43.8**^{W**,S*}	55.1	37.5
West	**40.0**^{E*}	49.4	**63.3**^{E**}	49.0	53.8
Mid-Canopy					
North	**38.5**^{W*}	**46.4**^{W*}	**65.7**^{W**}	85.1	62.7
South	42.9	**60.3**^{E*}	76.3	72.5	66.7
East	**28.6**^{W***}	**44.8**$^{W***, S*}$	**59.3**^{W**}	70.1	55.0
West	**64.3**$^{E***, N*}$	**77.3**^{E***,N*}	**82.0**$^{E**, N**}$	91.0	80.0
Canopy-Periphery					
North	69.2	83.8	83.3	90.2	82.7
South	69.2	82.5	93.2	**90.9**^{E*}	89.0
East	57.1	63.1	71.6	**78.6**^{S*}	66.1
West	68.4	75.0	85.7	83.3	83.3
Outside-of-Canopy					
North	71.4	81.5	90.0	91.6	88.2
South	71.4	82.8	90.0	92.3	89.0
East	71.4	83.7	92.3	92.5	88.0
West	78.9	88.6	92.3	94.6	90.7

ward to lee-ward *TF* ratios for each storm and for each sampling zone are shown in Figure 2.4, where it is evident that *DoSO* does have an influence on *TF* heterogeneity within each zone. Mean event ratios (n = 38) for all four zones significantly differed from unity: inner-canopy (1.55 ± 1.11, p = 0.0022); mid-canopy (1.49 ± 0.79, p = 0.0001); canopy-periphery (1.22 ± 0.38, p = 0.0004), and outside-of-canopy (1.15 ± 0.47, p = 0.0435).

Temporal stability of throughfall

Table 2.6 list the Spearman and Pearson correlation coefficients between cumulative *TF*% of the four different rain depth classes for the four sampling zones. In general, correlation coefficients were highest between cumulative *TF*% with similar rainfall depths. For example,

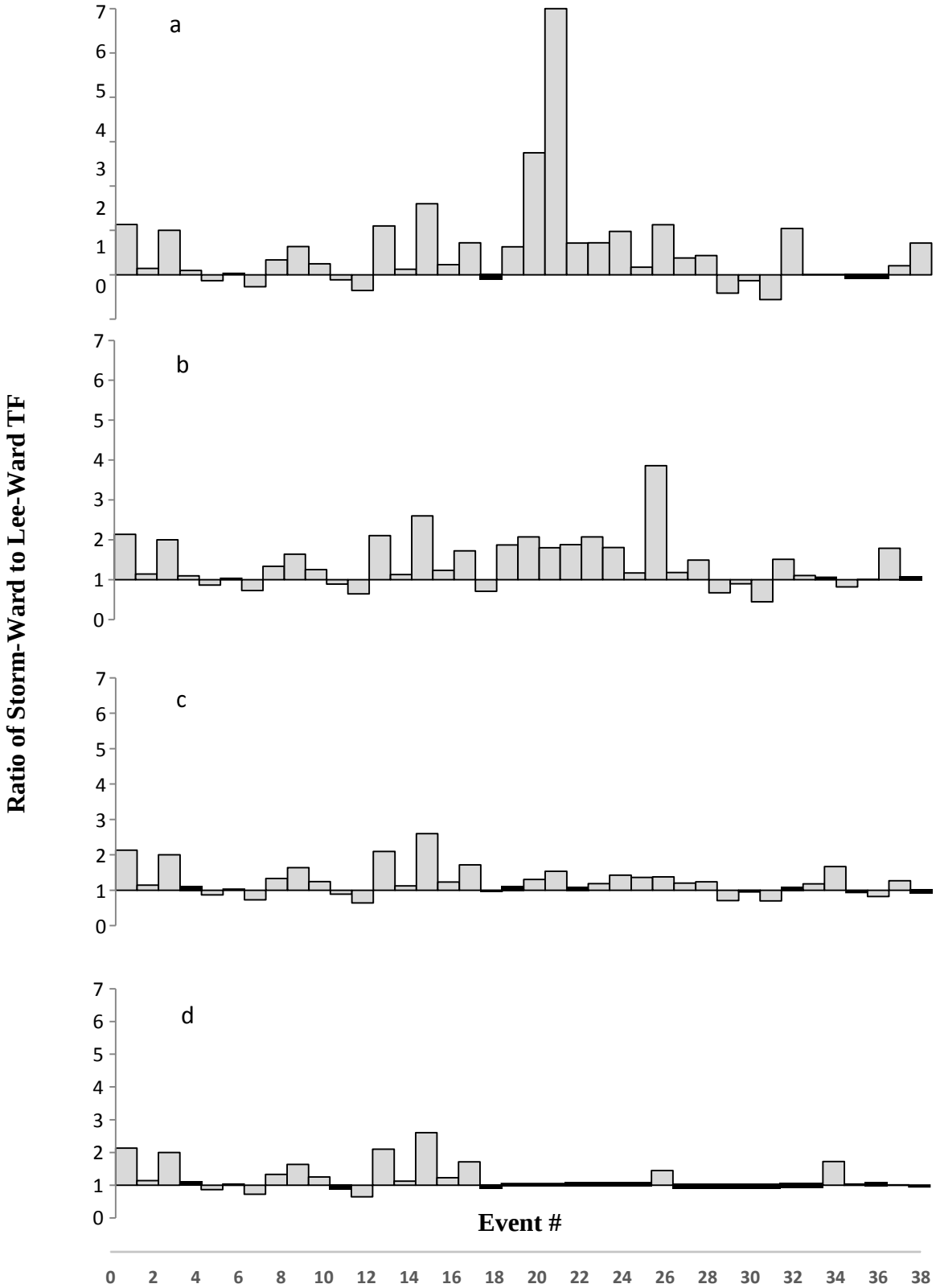

Figure 2.4: Ratio of event storm-ward to lee ward TF throughout the study period for the a) inner-canopy, b) mid-canopy, c) canopy-periphery, and d) outside-of-canopy sampling zones.

Table 2.6: Spearman (right) and Pearson (left) correlation coefficients between cumulative *TF*% of four different rain-depth classes (< 2, 2 to < 5, 5 to < 10, and ≥ 10 mm) for the four sampling zones (inner-canopy, mid-canopy, canopy-periphery, and outside-of-canopy) (n = 36, $^{*}p \leq 0.05$, $^{**}p \leq 0.01$; n.s. = not significant).

	Rain Depth Class		
	2 to < 5 mm	5 to < 10 mm	≥ 10 mm
Inner-Canopy			
< 2 mm	0.576^{**}, 0.654^{**}	0.633^{**}, 0.656^{**}	0.391^{*} , 0.347^{*}
2 to < 5 mm		0.806^{**}, 0.891^{**}	0.717^{**}, 0.695^{**}
5 to < 10 mm			0.776^{**}, 0.799^{**}
Mid-Canopy			
< 2 mm	0.869^{**}, 0.868^{**}	0.827^{**}, 0.791^{**}	0.524^{**}, 0.584^{**}
2 to < 5 mm		0.889^{**}, 0.853^{**}	0.554^{**}, 0.630^{**}
5 to < 10 mm			0.616^{**}, 0.771^{**}
Canopy-Periphery			
< 2 mm	0.719^{**}, 0.733^{**}	0.658^{**}, 0.597^{**}	0.484^{**}, 0.507^{**}
2 to < 5 mm		0.813^{**}, 0.793^{**}	0.742^{**}, 0.810^{**}
5 to < 10 mm			0.827^{**}, 0.848^{**}
Outside-of-Canopy			
< 2 mm	0.544^{**}, 0.550^{**}	0.387^{*} , 0.423^{*}	$0.149^{n.s.}$, $0.173^{n.s.}$
2 to < 5 mm		0.830^{**}, 0.831^{**}	0.573^{**}, 0.598^{**}
5 to < 10 mm			0.788^{**}, 0.797^{**}

the strongest correlations were found between the 2 to < 5 and 5 to < 10 mm rain-depth classes for the inner-canopy, mid-canopy, and outside-of-canopy zones (r_s ranging from 0.806 to 0.881, $p \leq 0.05$, r from 0.831 to 0.891, $p \leq 0.05$), while for the canopy-periphery zone the strongest correlations were found between the 5 to < 10 and ≥ 10 mm rain-depth classes ($r_s = 0.827$, $p \leq 0.05$; $r = 0.848$, $p \leq 0.05$). The weakest correlations were found between the < 2 mm and the ≥ 10 mm rain-depth classes under all four sampling zones with the correlations not being significant for the outside-of-canopy-zone.

Spearman rank coefficient values for *TF* for all event pairings were derived for each of the canopy zones. Significant ($p < 0.05$) positive r_s values occurred for 277 (39.4%), 309 (44.0%), 370 (52.6%), and 295 (42.0%) of the 703 event pairings for the inner-canopy, mid-canopy, canopy-periphery and outside-the-canopy zones, respectively. Significant negative pairing were also found for the inner-canopy, mid-canopy and outside-the-canopy zones, but comprised only 16 (2.3%), 9 (1.3%), and 4 (0.6%) of the pairings, respectively. No

significant negative r_s pairings were found for the canopy-periphery zone. Maximum positive r_s values for individual event pairings ranged from 0.839 for the canopy-periphery between events 12 and 19 to 0.891 for the inner-canopy between events 23 and 28, while maximum negative r_s values ranged from -0.232 (not significant) for the canopy-periphery (between events 17 and 36) to -0.620 for the inner-canopy (between events 12 and 20). Figure 2.5 shows the temporal stability plot with all gauges from all zones pooled. Twenty-nine (81%) and 4 (11%) of the 36 gauges comprising the lower quartile were found to have *extreme* temporal persistence following the ± 1 SD and 95% confidence limit criteria, respectively. *Extreme* temporally persistence of *TF* input was also observed in the upper quartile region with 16 of the 36 gauges (44%) meeting the ± 1 SD criterion; albeit no gauge met the 95% confidence limit criterion. No gauges meet either persistence criterion within the inter-quartile region and thus, no *general* persistence was identified. Gauges situated in the inner-canopy dominated the *extreme* temporally persistent low TFS_i values (69%), with the mid-canopy (24%) and canopy periphery (7%) comprising the rest (i.e., no outside-of-canopy gauges). Seventy-five percent of the gauges identified as exhibiting *extreme* temporal persistence in the upper quartile were located outside-the-canopy, with gauges situated in the canopy periphery (19%) and mid-canopy (6%) accounting for the remainder. One-hundred and five of the 144 gauges (73%) were found to have TFS_i values that differed from zero at the 95% confidence level; 52 (36%) below zero and 53 (37%) above.

Figure 2.6 shows the temporal stability plots when each canopy zone is considered separately. At the canopy zone scale the frequency of temporally persistent TFS_i decreases considerably compared to when all zones are pooled. This is especially the case for the outside-of-canopy, inner-canopy, and mid-canopy zones, with only 1 (3%), 1 (3%), and 2 (6%) of the gauges exhibiting *extreme* persistence (i.e., in the region of the upper and lower quartiles of the ranked sample points) using the ± 1 SD criterion, respectively. No gauges were found to have *extreme* persistence using the 95% confidence limit criterion in the three aforementioned zones. The presence of temporally persistent *TF* was greater in the canopy-periphery zone than the other canopy zones, but was not as prevalent as when all zones are pooled. Nine of the 36 gauges (25%) in the canopy-periphery zone were found to exhibit *extreme* persistence using the ± 1 SD criterion and none using the 95% confidence limit criterion. When each canopy zone is considered separately, no gauges with *general*

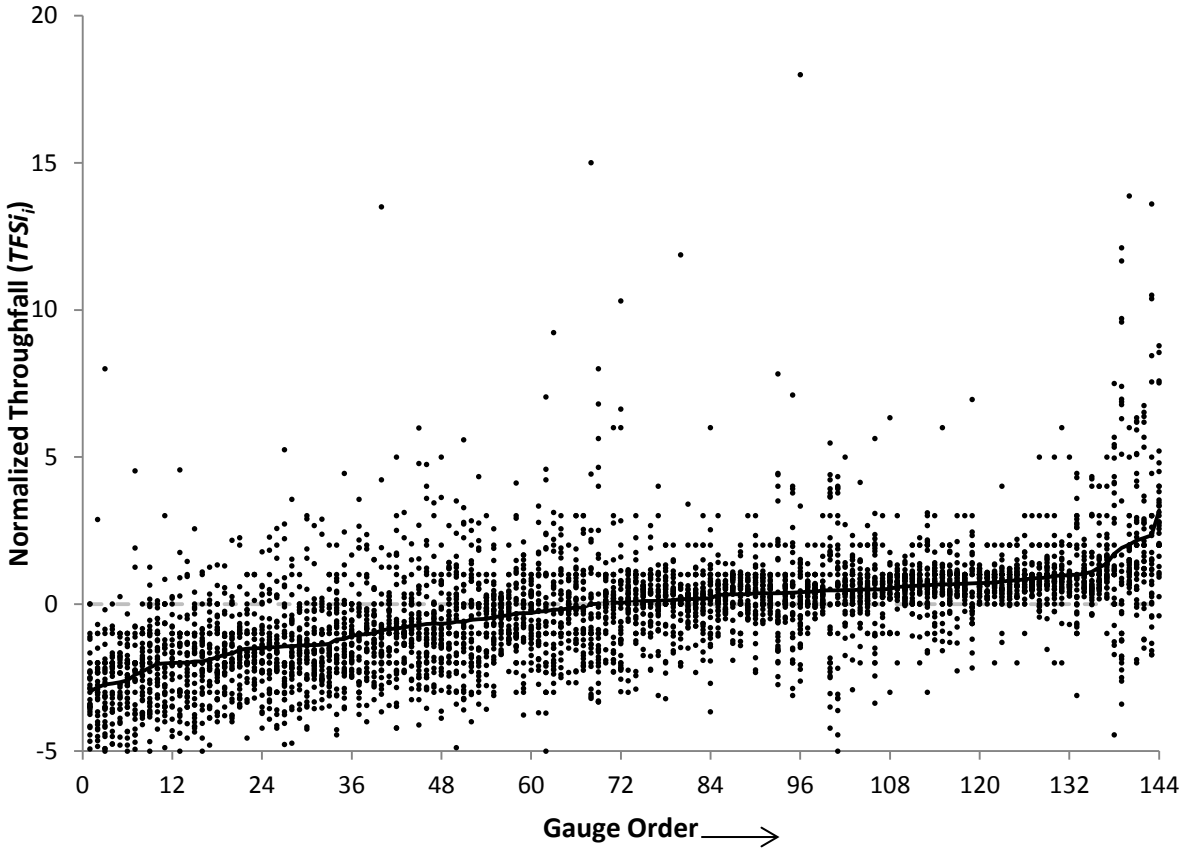

Figure 2.5: Temporal stability plot of normalized throughfall (TFS_i) for all 144 gauges. Individual dots represent event TFS_i values, while the solid line passes through the mean TFS_i value for all gauges ranked from lowest to highest mean TFS_i.

persistence (i.e., in the interquartile region of the ranked sample points) were found using either criterion. At the canopy-zone scale 20 (56%), 19 (53%), 21 (58%), and 22 (61%) of the 36 gauges in each the inner-canopy, mid-canopy, canopy-periphery, and outside-of-canopy zones, respectively, had individual mean TFS_i values that differed significantly ($p \leq 0.05$) from zero. Exceptionally large single-event deviations of TFS_i from the median (i.e., zero) were found. When all gauges are pooled, individual TFS_i values were as high as + 18.0 (Event 8, Tree 2, mid-canopy, north), while at the canopy sampling zone scale the maximum TFS_i value was + 25.3 (Event 26, Tree 2, inner-canopy, north). It is important to note that these two extreme values correspond to the same tree and transect.

When all gauges are pooled and when each of the canopy zones are analyzed separately the r_s of event pairings were found to be significantly ($p < 0.001$) negatively correlated to the temporal lag, Δday. However, the amount of variability in the r_s values of

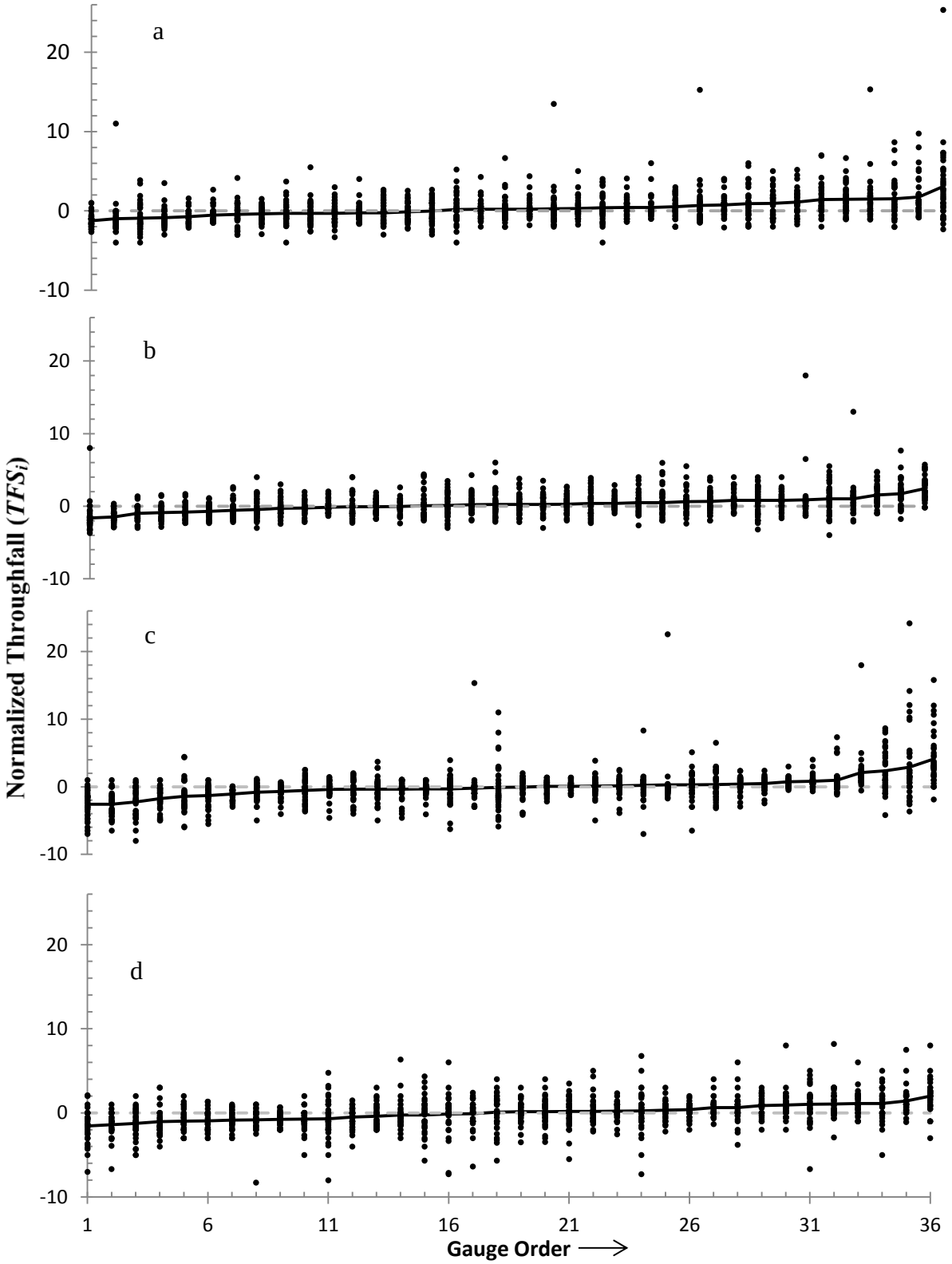

Figure 2.6: Temporal stability plots for the 36 gauges in each of the a) inner-canopy, b) mid-canopy, c) canopy-periphery, and d) outside-of-canopy sampling zones with median set to zero and unit variance (median absolute difference, MAD).

the event pairings explained was very low in each case ranging from $R^2 = 0.027$ for the outside-the-canopy zone to $R^2 = 0.078$ for the mid-canopy zone. For each canopy zone and when all gauges were pooled the addition of meteorological variables did increase the amount of variability in r_s explained (Table 2.7); however, a sizable portion of the variability remained unaccounted for with R^2 values only reaching 0.050 (inner canopy) to 0.130 (all gauges pooled).

DISCUSSION

Under all four lodgepole pine canopy zones *TF* % increased with increasing rain-depth class, in keeping with the findings of studies conducted for other trees or forest types (Gómez *et al*., 2002; Price and Carlyle-Moses, 2003; Ziegler *et al*., 2009; Fathizadeh *et al*., 2014). For the three below-canopy zones the increase in *TF* % with increasing rain depth likely reflects the gradually saturation of the canopy and the resultant fraction of rainfall reaching the ground as *TF* (Carlyle-Moses *et al*., 2004). For relatively small events, *TF* is comprised solely of, or is at least dominated by, free thoughfall – that is, *TF* that passes directly through gaps in the canopy (see Bringfelt and Härsmar, 1974; Gash 1979). With increasing rain input the water storage capacity of the canopy decreases and thus the contribution to *TF* in the form of canopy drip increases (Jackson, 1975; Carlyle-Moses *et al*., 2014). The lower median cumulative *TF* % values for the < 2 and 2 to < 5 mm rain depth classes for the inner- and mid-canopy zone compared with the canopy-periphery suggests that these sheltered areas closer to the tree bole have limited free thoughfall input and or require greater rain depths to generate sizable *TF* drip. Cumulative median *TF* % for the canopy-periphery was relatively high for small rain depth classes only increasing slightly under greater rain depth scenarios compared to the inner and mid-canopy. Additionally, no significant difference in cumulative *TF* % between the canopy-periphery or the mid-canopy was found for the ≥ 10 mm rain depth class. These findings suggests that, in general, the sparse canopy periphery is associated with relatively large free throughfall contributions and that the role of canopy drip *TF* at this zone is, for the most part, relatively minor compared with the inner- and mid-canopy. Additionally, because of the excurrent nature of the branching of these juvenile lodegpole pine trees, we speculate that drainage of intercepted rainfall from the canopy

periphery may move along branches inwards towards the tree bole (Ford and Deans, 1978). It should be noted that these observations are at the canopy-zone scale and not at the gauge scale as *TF* generated from canopy drip may result in individual gauges at the periphery and the other below canopy zones receiving relatively large and sometimes temporally persistent *TF* inputs.

The general pattern of *TF* increasing with increasing distance from the boles of juvenile lodgepole pine observed in this study is in agreement with observations reported for other trees (e.g., Aussenac, 1970; Johnson, 1990; Beier *et al*., 1993; Ito *et al*., 2008). However, this pattern is not universal with some researchers (e.g., Ford and Deans, 1978; Robson *et al*., 1994; Sato *et al*., 2011) finding the opposite to be true, that *TF* generally deceases with increasing distance from the bole. Some researchers found that the position of greatest *TF* input is located mid-way between the tree bole and the canopy periphery (Carleton and Kavanagh, 1990; Nanko *et al*., 2011), while others researchers found that no relationship between *TF* quantity and the position of the gauge relative to the tree bole exists (Loustau *et al*., 1992; Gómez *et al*., 2002; Loescher *et al*., 2002). Keim *et al*. (2005) found that the relationship between *TF* depth and distance to the nearest tree bole varied depending on species and age. We suggest that the pattern observed in this present study may be the result of a combination of factors, namely i) the isolated nature of the study trees with no overlap from other canopies, ii) the increase in canopy cover and, from casual observations in the field, the increase in the proportion of wood (which typically has a higher water storage capacity than foliage – see Herwitz, 1985; Llorens and Gallart, 2000) comprising that cover and the associated interception efficiency in the inner portions of the canopy compared with the periphery, and iii) although the excurrent branches may divert intercepted rainfall from the canopy periphery, the smoothness of these branches promotes flowall the way to the bole resulting in stemflow generation rather than canopy drip *TF*. The relatively large stemflow funneling ratios for juvenile lodgepole pines reported by McKee (2010) supports this assertion.

The increase in median cumulative *TF*% in the outside-of-canopy zone with increasing rain depth suggests that trees influence *TF* input beyond their projected canopy areas, confirming the results of others (e.g., King and Harrison, 1998; David *et al*., 2006).

Table 2.7: Coefficient values associated with meteorological factors influencing Spearman rank coefficient values of paired events and the intercept, and R^2 for each model for all gauges pooled and under each of the four canopy zones. (n = 703, $^{*}p \leq 0.05$, $^{**}p \leq 0.01$; $^{***}p \leq 0.001$).

Zone	Δday	ΔP	ΔD_E	ΔD_P	ΔI_{Mean}	ΔI_{Max30}	ΔN_B	ΔD_B	$\Delta DoSO$	Intercept	R^2
All Pooled	-0.001***	-	-	-	-0.025***	-0.012***	-	+0.004***	-0.0003*	+0.523***	0.130
Inner-canopy	-0.002***	-	-	-	-	-	-	+0.003**	-	+0.268***	0.050
Mid-Canopy	-0.002***	-0.004***	-	-0.006***	-	-0.012***	-	+0.004**	-	+0.384***	0.105
Canopy-Periphery	-0.001***	-0.004***	-	-	-	-	-	+0.002**	-	+0.422***	0.073
Outside-of-Canopy	-0.002***	-	-	-	-	-0.009**	+0.005*	-	-0.0007***	+0.421***	0.112

The interaction of the canopy with wind-driven rainfall can create rain-shadows in the lee-ward areas beyond the tree canopy (Herwitz and Slye, 1992; 1995; David *et al*., 2006). At a given wind speed, wind-driven rainfall will tend to be more inclined for events with lower rainfall depths since these events tend to be of lower intensity (in our study r_s between P and $I_{Mean} = 0.332$, $p = 0.0418$). The angle of inclination of rain falling at higher intensities is less affected by wind given the larger drop size and associated kinetic energy (Laws and Parsons, 1943). However, the lack of wind velocity data for our study limits any further conclusions regarding the role of the interaction of wind speed, rain depth and rain intensity. As stated by David *et al*. (2006), estimates of canopy interception loss from isolated trees using only below canopy gauges will violate the assumptions of mass balance and will result in an underestimate of the true interception efficiency of the tree(s) under wind-driven rainfall conditions.

As has been reported by others (e.g., Lin *et al.*, 1997; Rodrigo and Àvila, 2001; Vrugt *et al.*, 2003; Staelens *et al*., 2006), the *TF CV*% in the study stand as a whole and under all four canopy sampling zones decreased with increased rain depth up to a certain rain depth threshold. In this present study the variability of *TF* was significantly greater below tree canopies than in the areas between the canopies. Additionally, *TF* heterogeneity was significantly greater in the inner-and mid-canopies compared to the canopy-periphery. These findings suggest that canopy structure influences *TF* variability (see also Staelens *et al*., 2006; Nanko *et al*., 2011; Pypker *et al*., 2011; Sato *et al*., 2011); however, our results also suggest that the way in which canopy structure influences *TF* variability is complex. Although canopy cover fraction was significantly negatively correlated with *TF*% when all gauges were pooled, when each of the three below- canopy zones were considered separately only canopy cover fraction was negatively correlated with *TF*% in the mid-canopy zone under the two smallest rain depth classes. Additionally, tree size metrics, including tree height and basal area were not correlated to *TF*% for the inner-canopy zone, while they were for the mid-canopy zone for rain depth classes at or below 2 to < 5 mm and for the canopy-periphery for the ≥ 10 mm depth class. Thus, different canopy traits influence the partitioning of water into *TF* differently depending on location under the canopy (e.g., inner-canopy versus canopy-periphery) and the magnitude of the rain event, in agreement with the findings of Carlyle-Moses *et al*. (2004) in a mature pine-oak forest in northeastern Mexico.

Our results suggest that tree traits work in concert with meteorological factors in determining the spatial pattern of *TF* for a given storm. For example, *TF CV*% decreased with increasing 30-minute maximum rain intensity, the increasing duration of the event, and or the number and or duration of intra-storm breaks depending on the canopy sampling zone and or the rain depth class. We speculate that these storm variables, namely the 30-minute maximum rain intensity and intra-storm breaks, may influence *TF CV*% by reducing the development and or connectivity of flow paths (i.e., translocation) in the canopy, with these flow paths resulting in large drip points that increase *TF CV*% (see Herwitz, 1987; Carlyle-Moses and Price, 2006; Nanko *et al*., 2011; Sato *et al*., 2011). Others (e.g., Bouten *et al*., 1992; Raat *et al*., 2002) have also found that *TF CV*% decreases with some aspect of rainfall intensity, however, Hansen (1995) concluded, based on results from a Norway spruce forest in Denmark, that the amount of *TF* reaching different layers of the canopy remained approximately equal regardless of rainfall intensity, while Loescher *et al*. (2002) found, in an old-growth tropical forest, that *TF CV*% increased with increasing rain intensity. Thus, the influence of rainfall intensity on *TF CV*% seems to be dependent on some aspect of canopy structure and is not likely to be universal across all forest or tree types.

Direction of storm origin was found to have an important influence on *TF* quantity at the gauge scale, with *TF* typically being larger on the storm-ward side of the canopy than the lee-ward side for gauges in all four sampling zones. We suggest that this is the result of the probable relationship between the direction of storm origin and wind direction; however, the lack of wind speed and direction data for our study limits our interpretation of the processes involved. However, as aforementioned, wind-driven rainfall has been found to create rain-shadows on the lee-ward sides of trees in tropical forests (Herwitz and Slye, 1992; 1995) and Van Stan *et al*. (2011) found, in a temperate deciduous forest of the eastern United States, that preferential stemflow generation occurred during periods of inclined rainfall by wind from the east to north-northeast. These results, coupled with those of the present study, suggest that the spatial variability of understory precipitation is controlled, at least to some degree, by wind speed and direction and these variables should be evaluated in future studies on the controls on *TF* variability.

Temporal persistence of *TF* spatial patterns was found in this forest type as it has in others (e.g., Keim *et al*., 2005; Zimmermann *et al*., 2009; Sato *et al*., 2011; Carlyle-Moses *et*

al., 2014). A greater degree of persistence was found when all gauges were pooled compared to when canopy zones were evaluated separately. This finding is probably a consequence of the large differences in canopy trait characteristics between the zones. Persistence of median cumulative *TF* was greatest between rain depth classes of more similar magnitudes. At the event and gauge scale, however, persistence was much more variable reflecting the complex interaction of varying storm conditions with varying sub-canopy zone characteristics. In our study the maximum 30-minute rain intensity, duration of rain, direction of storm origin and the number and duration of storm breaks were found to be correlated with temporal stability for at least one of the zones or when all zones were pooled. Although spatial patterns were more similar with more alike maximum 30-minute intensity (in agreement with Zimmermann *et al*., 2008), rain duration and storm directions, the relationship between the number and duration of storm breaks was found to be opposite. That is, with greater dissimilarities in break periods and frequencies among events, the more similar the event spatial *TF* patterns. This finding suggests that, for our study at least, an increase in the number and or duration of storm breaks may dampen the degradation in temporal persistence resulting from differences in the magnitudes of other variables such as rain depth and the maximum 30-minute intensity. Nonetheless, much of the variability in the persistence of *TF* spatial patterns from one event to the next in this study was not explained. Again, wind speed and direction may be important factors that require future study.

The temporal persistence of *TF* variability in our study was found to marginally degrade with time across the study period, probably as a result of the slight changes to the canopy during growth across the time span of the study (five months). Zimmerman *et al* (2008) found that temporal persistence was much more sensitive to temporal lag in an open tropical rainforest in Brazil, especially during the early wet season when there was rapid vegetative growth. Zimmermann *et al*. (2008) also found that as the wet season progressed the degradation in temporal persistence was markedly reduced due to the more stable cover characteristics. Thus, our results coupled with the findings of Zimmermann *et al*. (2008) and others (e.g., Staelens *et al*., 2006) suggest that the temporal persistence of *TF* spatial patterns is strongly linked with the temporal dynamics of the canopy. The relatively minor influence of temporal lag on *TF* spatial patterns over the course of our study and the finding that a large number of gauges had associated median TFS_i values that significantly differed from zero

suggests that statistical independence of *TF* samples cannot be assumed in this stand if a stationary gauge approach is used (see Loescher *et al*., 2002; Carlyle-Moses *et al*., 2014).

CONCLUSION

The present study has found that *TF* is modified by the canopies of juvenile lodgepole pine in a systematic fashion, with this understory precipitation input typically increasing and its associated spatial heterogeneity decreasing with increasing distance from the tree bole. Tree and storm characteristics, such as tree size and direction of storm origin, were found to explain some of the variability in the spatial delivery of *TF*, however, the role of other variables that are likely drivers of this heterogeneity in this forest type, including wind speed and direction as well as wood cover, still need to be assessed.

Our results suggest that *TF* sampling in these juvenile forests be done with relatively denser networks of *TF* gauges in the inner- and mid-canopy zones as compared with the canopy-periphery and areas outside of the canopy due to the increased *TF* variability associated with the former zones. Areas outside of the canopy, however, are influenced by the canopies of juvenile pine, probably as a result of the effective catch of inclined rainfall, and thus need to be sampled. Sampling strategies should also take the prevailing direction of storm origin (or wind) into consideration. Given the degree of temporal persistence observed, it is recommended that *TF* gauges be periodically moved to different areas of the canopy so that assumptions of statistical independence are met.

The systematic nature of the spatial heterogeneity of *TF* and its temporal persistence suggests that directly or indirectly *TF* influenced hydrological, biogeochemical, and ecological aspects of these young forests may also have associated spatiotemporal trends. Further study to establish if such linkages exist is required. It is important to note that this study was conducted during the growing-season when rainfall dominates. Hydrological, biogeochemical and ecological processes may, however, be greatly influenced by the distribution of snow during the dormant season and the subsequent spatial patterns associated with snow melt. Thus, future studies should take the initial soil moisture pattern and subsequent changes to that pattern as a consequence of drainage and evapotranspiration into

account when assessing the influence of growing-season *TF* spatial patterns on hydro-ecological processes Additionally, spatiotemporal patterns in *TF* and associated hydro-ecological processes, if they exist, should be assessed at different stages of growth to determine the longevity of *TF* spatial patterns (i.e., to establish if the same *TF* spatial patterns persist over several growing seasons) and so that the impact of forest disturbance regimes, such as mountain pine beetle, and subsequent re-growth may be better understood.

REFERENCES

Aussenac G. 1970. Effect of forest cover on the ground distribution of rainfall. Annales des Sciences Forestières 27: 383-399.

BC Ministry of Forests and Range. 2008. Biogeoclimatic Ecosystem Classification Subzone/Variant Map for the Kamloops Forest District, Southern Interior Forest Region [map]. 1:250,000. Ministry of Forests and Range, Research Branch. Victoria, BC.

Bhat S, Jacobs J, Bryant M. 2011. The chemical composition of rainfall and throughfall in five forest communities: A case study in Fort Benning, Georgia. *Water, Air, & Soil Pollution* **218**: 323-332.

Bringfelt B, Härsmar P-O. 1974. Rainfall interception in a forest in the Velen hydrological representative basin: Treatment of data from the summer and autumn of 1973. *Nordic Hydrology* **5**: 146-165

Beier C, Hansen K, Gundersen P.1993. Spatial variability of throughfall fluxes in a spruce forest. En*vironmental Pollution* **81**: 257-267

Bouten W, Heimovaara TJ, Tiktak A. 1992. Spatial patterns of throughfall and soil water dynamics in a Douglas fir stand. *Water Resources Research* **28**: 3227-33

Carleton TJ, Kavanagh T. 1990. Influence of stand age and spatial location on throughfall chemistry beneath black spruce. *Canadian Journal of Forest Research* **20**: 1917-1925

Carlyle-Moses DE. 2004. A reply to R. Keim's comment on "Measurement and modelling of growing-season canopy water fluxes in a mature mixed deciduous forest stand, southern Ontario, Canada". *Agricultural and Forest Meteorology* **124**: 281-284

Carlyle-Moses DE, Flores Laureano JS, Price AG. 2004. Throughfall and throughfall spatial variability in Madrean oak forest communites of northeastern Mexico. *Journal of Hydrology* **297**: 124-135

Carlyle-Moses DE, Lishman CE, McKee AJ. 2014. A preliminary evaluation of throughfall sampling techniques in a mature coniferous forest. *Journal of Forestry Research* **25**: 407-413

Carlyle-Moses DE, Park AD, Cameron JL. 2010. Modelling rainfall interception loss in forest restoration trials in Panama. *Ecohydrology* **3**: 272-283

Carlyle-Moses DE, Price AG. 2007. Modelling canopy interception loss from a Madrean pine-oak stand, Northeastern Mexico. *Hydrological Processes* **21**: 2572-2580

Carlyle-Moses DE, Price AG. 2006. Growing-season stemflow production within a deciduous forest of southern Ontario. *Hydrological Processes* **20**: 3651-3663

Carlyle-Moses DE, Gash JHC. 2011. Rainfall Interception Loss by Forest Canopies. In: *Forest Hydrology and Biogeochemistry: Synthesis of Past Research and Future Directions*, Levia DF, Carlyle-Moses DE, Tanaka T (eds.). *Ecological Series* **216**, Springer-Verlag: Heidelberg, Germany; 407-423.

Cottam G, Curtis JT. 1956. The use of distance measures in phytosociological sampling. *Ecology* **37**: 451-460

David TS, Gash JHC, Valente F, Pereira JS, Ferreira MI, David JS. 2006. Rainfall interception by an isolated evergreen oak tree in a Mediterranean savannah. *Hydrological Processes* **20**: 2713-2726

Fathizadeh O, Attarod P, Keim RF, Stein A, Amiri GZ, Darvishsefat AA. 2014. Spatial heterogeneity and temporal stability of throughfall under individual Quercus brantii trees. *Hydrological Processes* **28**: 1124-1136

Ford ED, Deans JD. 1978. The effects of canopy structure on stemflow, throughfall and interception loss in a young sitka spruce plantation. *Journal of Applied Ecology* **15**: 905-917.

Gash JHC. 1979. An analytical model of rainfall interception in forests. *Quarterly Journal of the Royal Meteorological Society* **105**: 43-55

Gerrits AMJ, Pfister L, Savenije HHG. 2010. Spatial and temporal variability of canopy and forest floor interception in a beech forest. *Hydrological Processes* **24**: 3011-3025

Gómez JA, Vanderlinden K, Giráldez JV, Fereres E. 2002. Rainfall concentration under olive trees. *Agricultural Water Management* **55**: 53-70

Hansen K. 1995. In-canopy throughfall measurements in Norway spruce: Water flow and consequences for ion fluxes. *Water, Air and Soil Pollution* **85**: 2259-2264

Helvey JD, Patric JH. 1965. Canopy and litter interception of rainfall by hardwoods of eastern United States. *Water Resources Research* **1**: 193-206

Herwitz SR. 1987. Raindrop impact and water flow on the vegetative surfaces of trees and the effects on stemflow and throughfall generation. *Earth Surface Processes and Landforms* **12**: 424-432

Herwitz SR. 1985. Interception storage capacities of tropical rainforest canopy trees. *Journal of Hydrology* **77**: 237-252

Herwitz SR, Slye RE. 1995. Three-dimensional modeling of canopy tree interception of wind-driven rainfall. *Journal of Hydrology* **168**: 205-226

Herwitz SR, Slye RE. 1992. Spatial variability in the interception of inclined rainfall by a tropical rainforest canopy. *Selbyana* **13**: 62-71

Holwerda F, Scatena FN, Bruijnzeel LA. 2006. Throughfall in a Puerto Rican lower montane rain forest: A comparison of sampling strategies. *Journal of Hydrology* **327**: 592-602

Ito A, Onda Y, Nanko K, Fukuyama T, Moriwaki H. 2008. Experimental study on spatial distribution of throughfall under a Japanese cypress tree. *Journal of Japan Society of Hydrology and Water Resources* **21**: 273-284

Johnson RC. 1990. The interception, throughfall and stemflow in a forest in Highland Scotland and the comparison with other upland forests in the U.K. *Journal of Hydrology* **118**: 281-287

Keim, RF, Skaugset, AE, Weiler, M. 2005. Temporal persistence of spatial patterns in throughfall. *Journal of Hydrology* **314**: 263–274

Kimmins, JP. 1973. Some statistical aspects of sampling throughfall precipitation in nutrient cycling studies in British Columbian coastal forests. *Ecology* **54**: 1008-1019.

King BP, Harrison SJ. 1998. Throughfall patterns under an isolated oak tree. *Weather* **53**: 111–121

Konishi S, Tani M, Kosugi Y, Takanashi S, Sahat MM, Nik AR, Niiyama K, Okuda T. 2006. Characteristics of spatial distribution of throughfall in a lowland tropical rainforest, Peninsular, Malaysia. *Forest Ecology and Management* **224**: 19-25

Laws JO, Parsons DA. 1943. The relation of raindrop-size to intensity. *Transactions of the American Geophysical Union* **24**: 452-460

Levia DF, Keim RF, Carlyle-Moses DE, Frost EE. 2011. Throughfall and stemflow in wooded ecosystems. In: *Forest Hydrology and Biogeochemistry: Synthesis of Past*

Research and Future Directions, Levia DF, Carlyle-Moses DE, Tanaka T (eds.). *Ecological Series* **216**, Springer-Verlag: Heidelberg, Germany; 425-444.

Levy KJ. 1979. Pairwise comparisons associated with the *K* independent sample median test. *The American Statistician* **33**: 138-139

Lin T-C, Hamburg SP, King H-B, Hsia Y-J. 1997. Spatial variability of throughfall in a subtropical rainforest in Taiwan. *Journal of Environmental Quality* **26**: 172-180

Llorens P, Gallart F. 2000. A simplified method for forest water storage capacity measurement. *Journal of Hydrology* **240**: 131-144

Lloyd CR, Marques FA de O. 1988. Spatial variability of throughfall and stemflow measurements in Amazonian rainforest. *Agricultural and Forest Meteorology* **42**: 63-73

Loescher HW, Powers JS, Oberbauer SF. 2002. Spatial variation of throughfall volume in an old-growth tropical wet forest, Costa Rica. *Journal of Tropical Ecology* **18**: 397-407

Loustau, D, Berbigier, P, Granier, A, El Hadj Moussa, F. 1992. Interception loss, throughfall and stemflow in a maritime pine stand, II. An application of Gash's analytical model of interception. *Journal of Hydrology* **138**: 469–485

Macinnis-Ng CMO, Flores EE Muller H, Schwendenmann L. 2012. Rainfall portioning into throughfall and stemflow and associated nutrient fluxes: land use impacts in a lower montane tropical region of Panama. *Biogeochemistry* **111**: 661-67

Manderscheid B, Matzner E. 1995. Spatial heterogeneity of soil solution chemistry in a mature Norway spruce (Picea abies (L.) Karst.) stand. *Water, Air and Soil Pollution* **85**: 1185-1190

Mann HB, Whitney DR. 1947. On a test of whether one or two random variables is stochastically larger than the other. *Annals of Mathematical Statistics* **18**: 50-60

Marin CT, Bouten W. Savink J. 2000. Gross rainfall and its partitioning into throughfall, stemflow and evaporation of intercepted water in four forest ecosystems in western Amazonia. *Journal of Hydrology* **237**: 40-57

McKee AJ. 2010. The Quantitative Importance of Stemflow: An Evaluation of Past Research and Results from a Study in Lodgepole Pine (Pinus contorta var. latifolia) Stands in Southern British Columbia. M.Sc.Env.Sc. Thesis, Graduate Program in Environmental Science. 113.

Mood AM. 1950. *Introduction to the Theory of Statistics*. McGraw Hill: New York; 433.

Nanko K, Onda Y, Ito A, Moriwaki H. 2011. Spatial variability of throughfall under a single tree: Experimental study of rainfall amount, raindrops, and kinetic energy. *Agricultural and Forest Meteorology* **151**: 1173-1182

Návar J. 2013. The performance of the reformulated Gash's interception loss model in Mexico's northeastern temperate forests. *Hydrological Processes* **27**: 1623-1633

Parker, G.1983. Throughfall and stemflow in forest nutrient cycle. *Advances in Ecological Research* **13**, 57-103

Pedersen LB, 1992. Throughfall chemistry of Sitka spruce stands as influenced by tree spacing. *Scandinavian Journal of Forest Research* **7**: 433–444

Poppenborg P, Hölscher D. 2009. The influence of emergent trees on rainfall distribution in a cacao agroforest (Sulawesi, Indonesia). *Flora – Morphology, Distribution, Functional Ecology of Plants* **204**: 730-736

Price AG, Dunham K, Carleton T, Band L. 1997. Variability of water fluxes through the black spruce (Picea mariana) canopy and feather moss (Pleurozium schreberi) carpet in the boreal forest of northern Manitoba. *Journal of Hydrology* **196**: 310–323

Price AG, Carlyle-Moses DE. 2003. Measurement and modelling of growing-season canopy water fluxes in mature mixed deciduous forest stand, southern Ontario, Canada. *Agricultural and Forest Meteorology* **119**: 69-85

Puckett LJ. 1991. Spatial variability and collector requirements for sampling throughfall volume and chemistry under a mixed-hardwood canopy. *Canadian Journal of Forest Research* **21**: 1581-1588

Pypker TG, Levia DF, Staelens J, Van Stan II JT. 2011. Canopy Structure in Relation to Hydrological and Biogeochemical Fluxes. In: *Forest Hydrology and Biogeochemistry: Synthesis of Past Research and Future Directions*, Levia DF, Carlyle-Moses DE, Tanaka T (eds.). *Ecological Series* **216**, Springer-Verlag: Heidelberg, Germany; 371-388.

Raat KJ, Draaijers GPJ, Schaap MG, Tietema A, Verstraten JM, 2002. Spatial variability of throughfall water and chemistry and forest floor water content in a Douglas fir forest stand. *Hydrology and Earth System Science* **6**: 363-374

Reid LM, Lewis J. 2009. Rates, timing, and mechanisms of rainfall interception loss in a coastal redwood forest. *Journal of Hydrology* **375**: 459-470

Rice AV, Thormann MN, Langor DW. 2007. Mountain pine beetle associated blue-stain fungi cause lesions on jack pine, lodgepole pine, and lodgepole x jack pine hybrids in Alberta. *Canadian Journal of Botany* **85**: 307-315

Ritter A, Regalado CM. 2014. Roving revisited, towards an optimum throughfall sampling design. *Hydrological Processes* **28**: 123-133

Robson AJ, Neal C, Ryland GP, Harrow M. 1994. Spatial variations in throughfall chemistry at the small plot scale. *Journal of Hydrology* **158:**107– 22

Rodrigo A, Àvila A. 2001. Influence of sampling size in the estimation of mean throughfall in two Mediterranean holm oak forests. *Journal of Hydrology* **243**: 216-227

Sakamoto Y, Ishiguro M, Kitagawa G. 1986. *Akaike Information Criterion Statistics*. Reidel: Dordrecht, Netherlands; 290

Saito T, Matsuda H, Komatsu M, Xiang Y, Takahashi A, Shinohara Y, Otsuki K. 2013. Forest canopy interception loss exceeds wet canopy evaporation in Japanese cypress (Hinoki) and Japanese cedar (Sugi) plantations. *Journal of Hydrology* **507**: 287-298

Sato AM, de Souza Velar A, Netto, ALC.2011. Spatial variability and temporal stability of throughfall in a eucalyptus plantation in the hilly lowlands of southern Brazil. *Hydrological Processes* **25**: 1910-1923

Shapiro SS, Wilk MB. 1965. An analysis of variance test for normality (complete samples). *Biometrika* **52**: 591-611

Spittlehouse DL. 1998. Rainfall interception in young and mature conifer forests in British Columbia. *Proceedings of the 23rd Conference on Agricultural and Forest Meteorology*, 2-6 November 1998, Albuquerque, New Mexico: American Meteorological Society

Staelens J, Schrijver AD, Verheyen K, Verhoest N. 2006. Spatial variability and temporal stability of throughfall water under a dominant beech (Fagus sylvatica L.) tree in relationship to canopy cover. *Journal of Hydrology* **330**: 651-662

Stout B, McMahon J. 1961. Throughfall variation under tree crowns. *Journal of Geophysical Research* **66**: 1839-1843

Uunila L, Guy B, Pike R. 2006. Hydrologic effects of mountain pine beetle in the interior pine forests of British Columbia: Key questions and current knowledge. *Journal of Ecosystems and Management* **7**: 37-40

Vachaud G, Passerat De Silans P, Balabanis P, Vauclin M. 1985. Temporal stability of spatially measured soil water probability function. *Soil Science Society of America Journal* **49**: 822-828

Van Stan II JT, Stiegert CM, Levia DF, Scheick CE. 2011. Effects of wind-driven rainfall on stemflow generation between codominant tree species with differing crown characteristics. *Agricultural and Forest Meteorology* **151**: 1277-1286

Vrugt JA, Dekker SC, Bouten W. 2003. Identification of rainfall interception model parameters from measurements of throughfall and forest canopy storage. *Water Resources Research* **39**: 1259

Wang, T, Hamann A, Spittlehouse DL, Aitken SN. 2006. Development of scale-free climate data for Western Canada for use in resource management. *International Journal of Climatology* **26**: 383-397.

Wang T, Hamann A, Spittlehouse DL, Murdock QT. 2012. ClimateWNA—High-resolution spatial climate data for Western North America. *Journal of Applied Meteorology and Climatology* **51**: 16-29

Wullaert H, Pohlert T, Boy J, Valarezo C, Wilcke W. 2009. Spatial throughfall heterogenity in a montane rain forest in Ecuador: Extent, temporal stability and drivers. *Journal of Hydrology* **377**: 71-79

Zar JH. 1984. *Biostatistical Analysis* (2nd Edition). Prentice hall: Englewood Cliffs, New Jersey; 718

Ziegler AD, Giambelluca TW, Nullet MA, Sutherland RA, Tanatasarin C, Vogler JB, Negishi JN. 2009. Throughfall in an ever-green dominated forest stand in northern Thailand: Comparison of mobile and stationary methods. *Agricultural and Forest Meteorology* **149**: 373-384

Zimmermann A, Germer S, Neill C, Krusche AV, Elsenbeer H. 2008. Spatio-temporal patterns of throughfall and solute deposition in an open tropical rainforest. *Journal of Hydrology* **360**: 87-102

Zimmermann A, Wilcke W, Elsenbeer H. 2007. Spatial and temporal patterns of throughfall quantity and quality in a tropical montane forest in Ecuador. *Journal of Hydrology* **343**: 80-96

Zimmermann A, Zimmermann B. 2014. Requirements for throughfall monitoring: The roles of temporal scale and canopy complexity. *Agricultural and Forest Meteorology* **189-190**: 125-139

Zimmermann B, Zimmermann A., Elsenbeer H. 2009. Rainfall redistribution in a tropical forest: Spatial and temporal patterns. *Water Resources Research* **45**: W011413

Zimmermann B, Zimmermann A., Lark R.M, Elsenbeer H. 2010. Sampling procedures for throughfall monitoring: A simulation study. *Water Resources Research* **46**: W01503. DOI: 10.1029/2009WR007776.

Zirlewagen D, von Wilpert K. 2001. Modeling water and ion fluxes in a highly structured, mixed-species stand. *Forest Ecology and Management* **143**: 27-37

CHAPTER 3
ANALYTICAL MODELLING OF CANOPY INTERCEPTION LOSS FROM A JUVENILE LODGEPOLE PINE (*Pinus contorta* var. *latifolia*) STAND

INTRODUCTION

In the central interior of British Columbia (BC), Canada, the mountain pine beetle (*Dendroctonus ponderosae* Hopkins) (MPB) has severely affected the majority of pine species in the region, but none more than the lodgepole pine (*Pinus contorta* Douglas ex Louden var. *latifolia* Engelm. ex S. Watson). By 2004, more than seven million hectares of lodgepole pine forests were infested by MPB in BC (Rice *et al*., 2007). The loss of mature lodgepole pine stands, including those lost to salvage logging, has resulted in an increase in the number of juvenile pine stands in the interior of BC through planting and natural regrowth. With this change from mature forests to juvenile forests at such a large spatial scale, the water balance of impacted areas may be altered, although the magnitude of such change is uncertain. For example, juvenile stands produce more stemflow - intercepted rainfall that is diverted to the base of trees by flowing along branches and down the boles of trees - than do mature stands (Spittlehouse, 1998; McKee and Carlyle-Moses, 2010). In addition, with the decrease in canopy cover, throughfall - rainfall that either passes directly through canopy gaps or as canopy drip -will likely be greater in juvenile stands compared to their mature counterparts. Given the scale of the MPB infestation, there is a need to quantify the hydrology of these juvenile stands and to simulate various components of the hydrologic cycle, including throughfall, stemflow, and canopy interception loss (I_c) - the proportion of rainfall that is intercepted, stored and subsequently evaporated from the forest canopy.

Canopy interception loss, I_c, from mature lodgepole pine forests or stands that comprise lodgepole pine with other species is appreciable, accounting for 24 – 29% of season-long rainfall (Spittlehouse, 1998; Moore *et al*., 2008), falling in the mid to upper range of the span of 10 – 50% for forest canopies across the globe reported by Roth *et al*. (2007). Given the relatively sparse canopy and low stand stature, and thus decreased aerodynamic conductance of juvenile lodgepole pine stands compared to their mature counterparts, I_c likely represents a smaller fraction of seasonal rainfall than from mature forests. This difference of I_c is further supported by a large difference in leaf area index (LAI). Coops et al., (2009) found in a 90-100 year old lodgepole stands in southeastern BC,

the LAI ranged from 2.83 to 8.0, whereas, in juvenile lodgepole pine (12 years old) near Prince George resulted in a LAI of 1.5 (Dhar et al., 2015). However, in the absence of an I_c study in a juvenile lodgepole pine environment the quantitative impact of the transition from mature to juvenile stands on I_c cannot be expressed with any degree of certainty.

Since I_c has often found to be of a quantitative importance a number of simulation models have been developed to model this component of landscape evaporation. The Gash analytical model (Gash, 1979) and its subsequent revisions (Gash *et al*. 1995; Valente *et al*. 1997) is the most commonly applied I_c model (Muzylo *et al*. 2009; Carlyle-Moses and Gash 2011). The Gash model represents a compromise between the overly simplistic linear regression approach (e.g., Helvey and Patric 1965) that is only representative of the forest community from which measurements were made, and the data-demanding, physically-based numerical model of Rutter et al. (1971; 1975). A review of the I_c literature suggests that 16 studies have been conducted to date that have evaluated the Gash model or its reformulations in coniferous forests. However, the Gash model has yet to be applied to lodgepole pine forests and none of the 16 studies assessed the model under juvenile coniferous conditions.

The Gash analytical model follows the 'water box approach' in which drainage is assumed to occur only when the canopy storage capacity, S_c has been satisfied. Once S_c has been exceeded additional rainfall is partitioned into during-event evaporation, canopy drip throughfall, or is directed to the boles of the trees where it may become stored, evaporated during rainfall, or reach the forest floor as stemflow. Canopy storage is assumed to remain constant once a certain threshold rainfall depth has been reached and does not increase with additional rainfall input. However, the physical basis of the 'water box approach' has been questioned (e.g., Klaasen *et al*. 1998), with many interception loss studies (e.g., Aston 1979; Calder 1990) suggesting that S_c increases in an exponential fashion with increasing rainfall. The gradual wetting of the canopy, through processes such as the relatively slow saturation of the underside of leaves compared with the upper-sides and raindrops splashing onto already wetted components of the canopy, will be referred to as the 'exponential wetting approach' for the remainder of this thesis. Interception loss models that follow the 'exponential wetting approach' permit drainage (throughfall and stemflow) from unsaturated canopies, unlike the 'water box approach'. Liu (1997) derived an analytical exponential wetting model which, like the Gash model, has been found to generate I_c values that are in

good agreement with observed values in a number of vegetation communities (see Liu, 2001; Carlyle-Moses and Price 2007). The Liu model was reformulated by Carlyle-Moses and Price (2007) to simulate sparse-canopy I_c in much the same way Gash *et al*. (1995) and Valente *et al*. (1997) reformulated the Gash model for the same purpose.

The objectives of this study, were to i) determine the quantitative importance of throughfall, stemflow and I_c, ii) evaluate the performance of the reformulated Gash (Valente *et al*. 1997) and reformulated Liu (Carlyle-Moses and Price, 2007) I_c models at both event and season-long time scales, and iii) assess the relative importance of during rainfall event evaporation and storage as components of canopy interception loss from these young forests.

MATERIALS AND METHODS

Research Site

Research was conducted at the Mayson Lake hydrological research area, which is located on the Thompson-Bonaparte plateau approximately 60 km NNW of Kamloops, British Columbia, Canada (51°12'49" N 120°23'43" W, 1290 m a.m.s.l.) (Figures 3.1 and 3. 2). The plot selected for this study was harvested in 1999 and planted with lodgepole pine seedlings within the following 2 years. Point quarter analysis revealed that in 2010 the plot (2600 m^2) was dominated by lodgepole pine with 5640 stems ha^{-1}, and a basal area of 9.6 m^2 ha^{-1}, while subalpine fir represented 980 stems ha^{-1}, and a basal area of 0.6 m^2 ha^{-1}. No other tree species occurred in the plot. Average lodgepole pine tree height was ~ 2.2 m (median ~1.7 m), with a maximum height of 5.2 m, while the average projected crown area (PCA) of these pines was ~ 0.9 m^2 (median ~ 0.5 m^2), with a maximum of 3.2 m^2. The total PCA of the plot was ~ 4940 m^2 ha^{-1}.

The study area has a mean annual precipitation depth of ~ 559 mm and temperature of 2.7 ^oC, with mean monthly temperatures ranging from -7.2 to 14.8 ^oC (Winkler et al., 2010). Rain is the dominate form of precipitation from mid-April through late September, with snow dominating the rest of the year (Figure 3.3). The Köppen climate classification for the region is Dfc (sub- arctic) while the provincial Biogeoclimatic Ecosystem Classification designation is Montane Spruce (dm3: North Thompson, dry mild variant) (B.C. Ministry of Forests and Range, 2008).

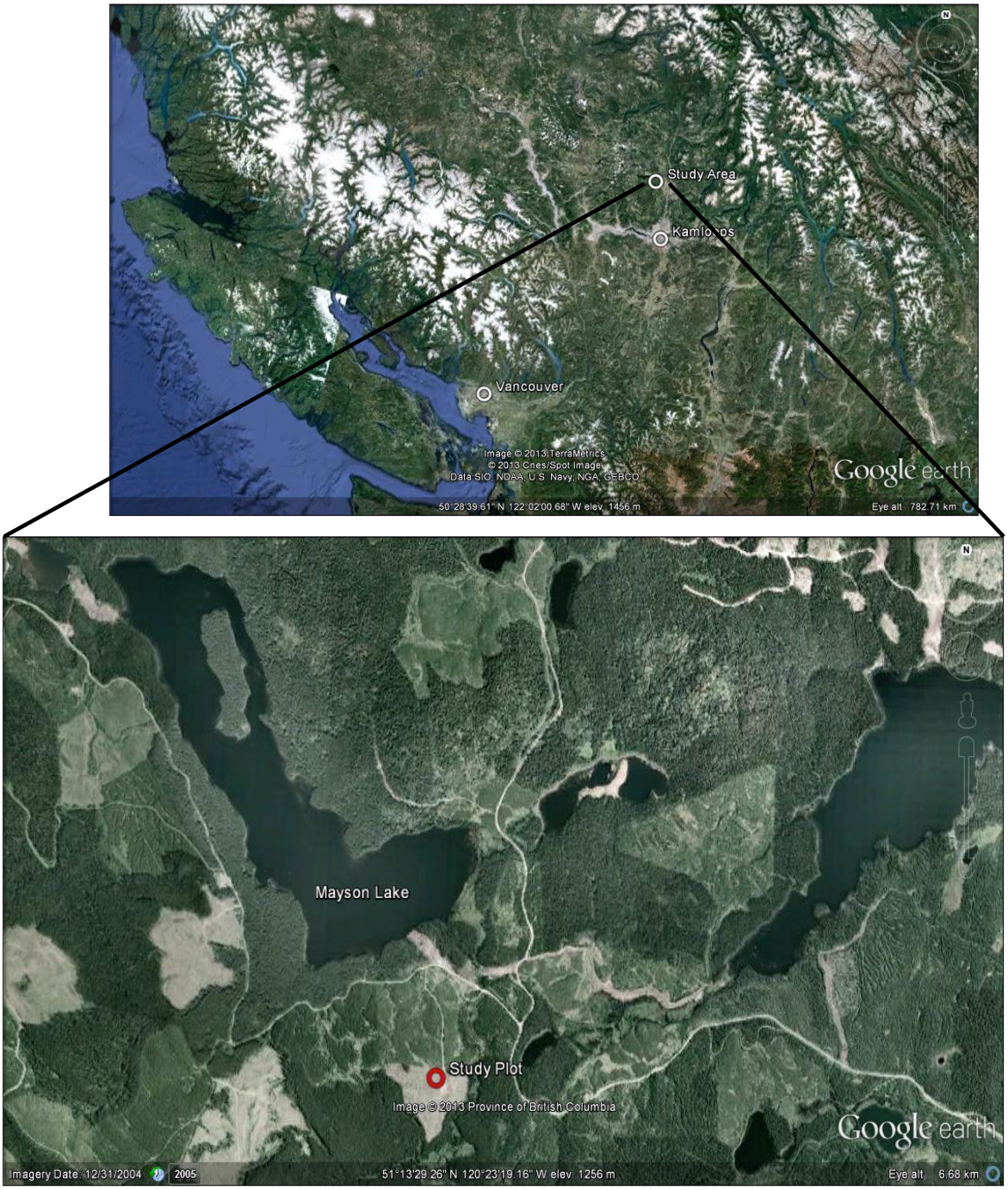

Figure 3.1: Geographic location of study plot.

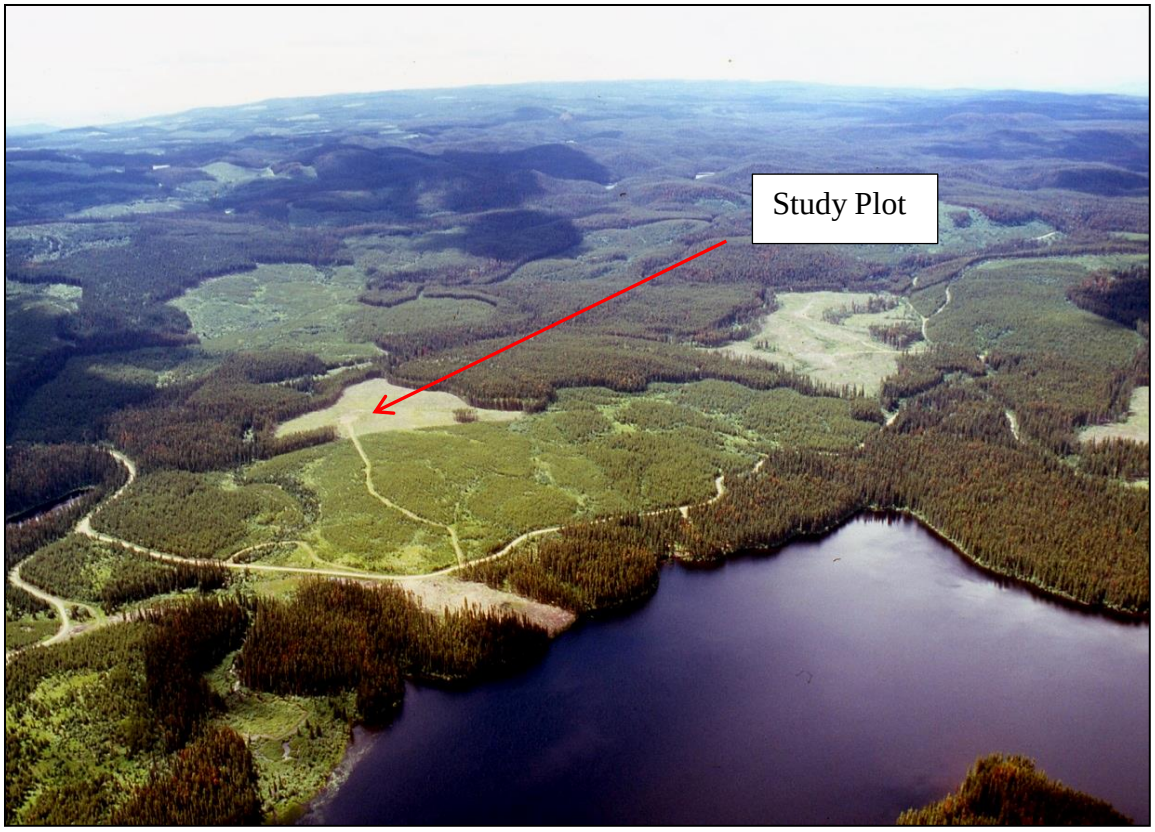

Figure 3.2: Aerial view of the study plot. Photo Credit: R.D. Winkler.

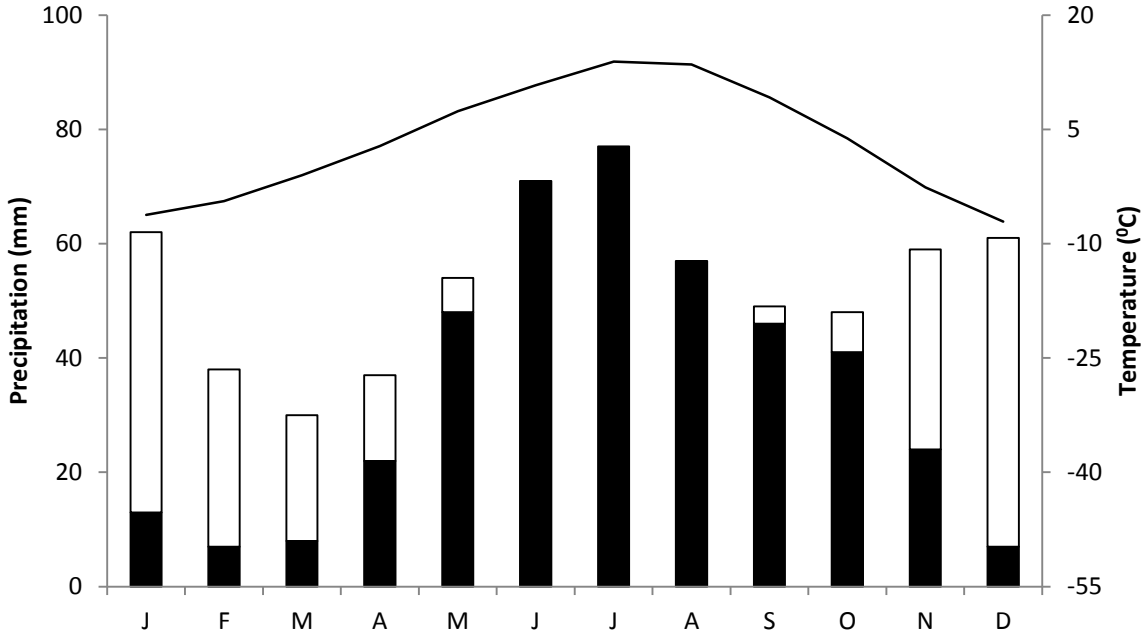

Figure 3.3: Climograph of study area based on ClimateBC ver 4.72 results using study plot latitude, longitude and elevation as inputs. Note: White bars = snow, black bars = rain.

Rainfall, Throughfall and Stemflow Measurement

Rainfall duration and intensity data were measured on an event basis from May 16 – September 30, 2010 using an Onset® tipping bucket rain gauge (model # S-RGB-M002) with a diameter of 15.4 cm and a resolution of 0.2 mm tip^{-1}. Additionally, rainfall depth was measured with a Meteorological Service of Canada Type-B rain gauge (diameter = 11.3 cm). The tipping bucket and the Type-B gauge openings were situated at a height of 1 m above the ground surface, located ~ 40 m south-west of the site (Figure 3.4). For this study a rain event was defined as a period of rainfall bounded by periods of 8 hours with no measurable rainfall as indicted by the tipping bucket rain gauge or evidence of rainfall from radar imagery compiled by Environment Canada's National Climate Data and Information Achieve[1], as this was the observed maximum time required for the boles and canopies to dry.

Figure 3.4: The Onset® tipping bucket rain gauge (left) and Meteorological Service of Canada Type-B rain gauge (right) used in this study

[1] See historical radar imagery at: http://www.climate.weatheroffice.gc.ca/radar/index_e.html?RadarSite=XSS&sYear=2013&sMonth=4&sDay=1&sHour=11&sMin=00&Duration=2&ImageType=Default

Throughfall was measured on an event basis under the canopies of nine trees whose characteristics are provided in Table 2.1. For each tree 16 manually-read Tru-Chek® wedge gauges (catch area = 36.3 cm^2 each) were used, with four of these gauges placed along four transects (N, W, S, E). Along each transect one gauge was placed adjacent to the tree base, one at the mid-canopy point, one at the canopy edge and the fourth gauge situated at a random distance in the open area between tree canopies, but within 45˚ of the top of the selected tree (Figure 3.5).

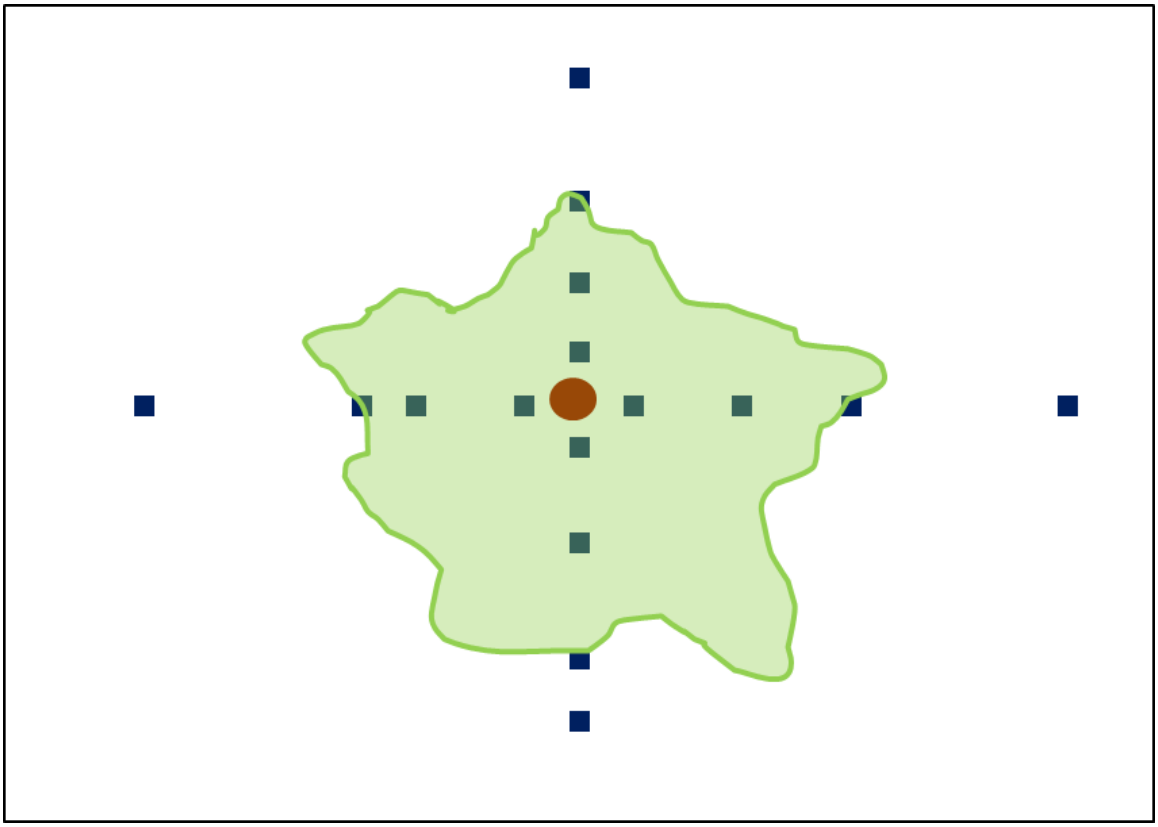

Figure 3.5: Throughfall gauge layout schematic. Shaded green = tree canopy, brown circle = tree bole, and blue squares = throughfall gauges.

Throughfall below each tree was estimated by taking the area-weighted average of each of the three below canopy zones (adjacent to tree, mid-canopy and canopy edge):

$$TF_T = \frac{1}{A}\sum_{z=1}^{z} a_z \cdot \overline{TF_z} \qquad (3.1)$$

where, TF_T is total below canopy throughfall (mm), A is the total area (m^2) beneath the tree canopy, a_z is the area of the below canopy zone (m^2), and $\overline{TF_z}$ is the mean throughfall catch (mm) within the below canopy zone.

Plot-scale below canopy throughfall at the rainfall event scale was estimated using one of two methods depending if there was a significant ($p < 0.10$) relationship between TF_T and tree size (basal area). For those events in which a relationship between TF_T and basal area was found, plot-scale below canopy throughfall was estimated by applying this relationship to the tree basal area frequency distribution collected as part of the point quarter exercise. For rainfall events where no significant relationship between TF_T and basal area could be found, mean below canopy throughfall for the plot was simply estimated as the average below canopy throughfall of the nine study trees. Finally, plot-scale throughfall was found by taking the sum of the area weighted plot-scale below canopy throughfall and the area weighted open area throughfall.

Stemflow was measured using the bottom of the two liter pop bottle to create a plastic collar, which we then sealed to the base of the tree with silicone. A small ~1cm diameter tube was inserted between the stemflow collar and the base of the tree to transfer the stemflow to either a tipping bucket rain gauge or a four liter storage device. Collected stemflow was measured after each event using a graduated cylinder. All stemflow collars were tested on a weekly basis and repaired if needed. Plot-scale stemflow at the rainfall event scale was estimated using the approach used to scale throughfall; with plot-scale stemflow found by applying a linear regression of tree-scale stemflow versus tree basal area for events in which a significant ($p < 0.10$) relationship between stemflow and tree basal area was found, and by taking the average stemflow of the sampled trees for events in which no significant relationship between stemflow and tree size was found. Figure 3.6 shows a stemflow collar + reservoir alongside the throughfall gauges for one of the study trees.

Plot-scale I_c was derived from the measured rainfall and calculated plot-scale throughfall and stemflow values using:

$$I_c = P_g - (TF + SF) \tag{3.2}$$

Figure 3.6: Stemflow and throughfall collection system for one of the selected study trees.

where, P_g is incident precipitation (mm) falling on the canopy and *TF* and *SF* are the plot-scale throughfall and stemflow inputs (mm) below the canopy.

Modeling Procedure

Rainfall interception loss, throughfall and stemflow were modeled using the reformulated Gash model (Valente *et al*. 1997) and reformulated Liu model (Carlyle-Moses and Price 2007). The Gash model is an analytical simulation tool that combines the conceptual framework of the sparse Rutter model (see Valente *et al*. 1997), including the division of a plot area into covered and uncovered sub-areas, with the ease of empirical equations. The sparse Gash model, like the original, considers that interception loss follows three phases for

discrete rainfall events: 1) the wetting-up of the canopy phase, 2) the saturated canopy phase, and 3) the canopy drying phase.

The various components of I_c as well as throughfall and stemflow were derived using the sparse Gash model and their formulations are provided in Table 3.1. The parameter values for the Gash model were derived following the methods outlined in Valente *et al*. (1997). The mean rainfall rate falling on a saturated canopy [R(mm h^{-1})] was determined from 36 event rainfalls during the study period. The mean evaporation rate from a saturated canopy was determined by using Gash's (1979) method:

$$E = a\,R \tag{3.3}$$

where, *a* is the slope of the canopy interception loss (mm), versus incident precipitation (> 0.5mm) linear regression.

Valente *et al*. (1997) use a modified envelope curve approach for determining the canopy storage capacity [S (mm)]. In addition, Valente *et al*. (1997) determined the drainage partitioning coefficient (P_d), as well as the trunk storage capacity [S_t (mm)] which are used the reformulated Gash model. Parameters *E*, *S*, and S_t are scaled to the fractional cover *c*: E_c, S_c, and S_{tc}. The parameter constant ε, which relates the evaporation rate of trunks to the saturated canopies, was estimated based on Valente *et al*. (1997) and Price and Carlyle-Moses (2003).

The depth of rainfall required to satisfy the canopy storage capacity [(Pg' (mm)] and trunk storage capacity [($Pg"=$ (mm)] were determined using the following formulas:

$$Pg' = -\frac{R}{(1-\varepsilon)\mathrm{Ec}}\,\frac{S}{c}\ln\left[1-\frac{(1-\varepsilon)\mathrm{Ec}}{R}\right] \tag{3.4}$$

$$Pg" = -\frac{R}{R-(1-\varepsilon)\mathrm{Ec}}\,\frac{S\mathrm{t}}{Pdc} + Pg' \tag{3.5}$$

Once all of the climatic and stand parameters have been determined the Valente *et al*. (1997) modified sparse Gash model formula can be used to calculate the interception loss:

Table 3.1: Components of canopy interception loss, throughfall and stemflow in the sparse Gash model. Adapted from Valente *et al*. (1997).

Component of Interception Loss	**Formulation**
Amount of incident P_g required to saturate the canopy ($P_g^{'}$)	$-\frac{\bar{R}}{(1-\epsilon)\bar{E}_c}\frac{S}{c}ln\left[1-\frac{(1-\epsilon)\bar{E}_c}{\bar{R}}\right]$
Amount of incident P_g required to saturate the trunks ($P_g^{''}$)	$\frac{\bar{R}}{\bar{R}-(1-\epsilon)\bar{E}_c}\frac{S_t}{p_d c}+P_g^{'}$
Interception loss from the canopy for *m* small storms insufficient to saturate the canopy ($P_g < P_g^{'}$)	$c\sum_{j=1}^{m}P_{g,j}$
and from the canopy for *n* storms large enough to saturate the canopy ($P_g \geq P_g^{'}$)	$c\left[nP_g^{'}+\frac{(1-\epsilon)\bar{E}_c}{\bar{R}}\sum_{j=1}^{n}\left(P_{g,j}-P_g^{'}\right)\right]$
Interception loss from the trunks for *q* storms that saturate the trunks ($P_g \geq P_g^{''}$)	qS_t
and from *n*-*q* storms that do not saturate the trunks ($P_g < P_g^{''}$)	$p_d c\left[1-\frac{(1-\epsilon)\bar{E}_c}{\bar{R}}\right]\sum_{j=1}^{n-q}\left(P_{g,j}-P_g^{'}\right)$
Stemflow	$p_d\cdot c\left[1-\frac{(1-\epsilon)\bar{E}_c}{\bar{R}}\right]\sum_{j=1}^{q}\left(P_{g,j}-P_g^{'}\right)-q\cdot S_t$
Throughfall	$(1-c)\sum_{j=1}^{m+n}P_{g,j}+(1-p_d)c\left[1-\frac{(1-\epsilon)\bar{E}_c}{\bar{R}}\right]\cdot\sum_{j=1}^{n}\left(P_g-P_g^{'}\right)$

Note: $\bar{R}$ is the mean rainfall intensity (mm h^{-1}) falling on a saturated canopy, $\bar{E}_c$ is the average evaporation rate of intercepted rainfall (mm h^{-1}) from a saturated canopy on a per unit area of canopy basis, *S* is the canopy storage capacity (mm), *c* is the canopy cover fraction, ϵ is the ratio of the evaporation rate from the trunks to that of the canopy, S_t is the storage capacity of the trunks (mm), and p_d represents the trunk partitioning coefficient.

$$c\sum_{j=1}^{m}Pg+\left[c\left\{nPg'+\frac{(1-\varepsilon)\mathrm{Ec}}{R}\sum_{j=1}^{n}(Pgj-pg')\right\}\right]+qS+$$
$$Pdc\left\{1-\frac{(1-\varepsilon)Ec}{R}\right\}x\sum_{j=1}^{n-q}(Pgj-Pg')j \qquad (3.6)$$

where, *m*, *n* and *q* represent the number of storms that do not saturate the canopy, that do saturate the canopy and that saturate the trunks, respectively.

The version of the Liu (1997) model used in this study was the analytical single-storm form since the canopy was assumed to be completely dry before each rainfall event. The

cumulative interception loss estimate is given as the sum of the single-storm estimates. The single-storm form of the Liu (1997) model is:

$$Ic = Cm\ \left[1 - \exp\left(-\frac{1-p}{cm}\right) Pg\right]\ x\ \left[1 - \left(\frac{E}{(1-p)R}\right)\right] + \frac{E}{R}\ Pg \quad (3.7)$$

where C_m is the stand storage capacity (mm), including the storage capacities of the canopy and trunks (i.e. $S_c + S_t$), p is the free throughfall coefficient, which represents the proportion of throughfall that reaches the forest floor by passing directly through the canopy and is regularly represented as $p = 1- c$ (Valente *et al*. 1997) .

Assuming $p = 1- c$, Eq. 6 can be rewritten for simulating I_c from sparse forests using the nomenclature of the reformulated Gash model (Carlyle-Moses and Price 2007):

$$Ic = c\ \left[Cmc\left[1 - \exp\left(-\frac{1}{Cmc}\right) Pg\right]\ x\ \left[1 - \left(\frac{Ec}{R}\right)\right] + \frac{Ec}{R} Pg\right] \quad (3.8)$$

where, C_{mc} is the storage capacity per unit area of the canopy + trunks (i.e. $S_c + S_t$).

Statistical Analysis and Model Evaluation

Statistical analysis and modeling was performed and analyzed using Microsoft® Office Excel 2007 (Microsoft Corporation, Redmond, WA, USA) and Smith's Statistical Package version 2.80. Excel 2007 was used for graphing and data organization and manipulation, while Smith's Statistical Package was used for linear regression analysis. A $p < 0.05$ level of statistical significance was used in this study. Model performance was assessed using coefficients of determination of observed versus simulated I_c values and the root mean square (RMSE) statistic (Mayer and Butler 1993; Carlyle-Moses *et al*. 2010):

$$RMSE = \sqrt{\frac{1}{n} + \sum_{i=1}^{n} (Ico_i - Icm_i)^2} \quad (3.9)$$

where, *Ico* and *Icm* represent the *i*th pair of observed and modeled Ic (mm) values, respectively.

The performance of the interception models were also assessed using the Nash-Sutcliffe criterion, which represents a measure of the variance of the observed data explained by the model (Ladson 2008):

$$C = \frac{\sum_{i=1}^{n}(O_i-\bar{O})^2 - (M_i-O_i)^2}{\sum_{i=1}^{n}(O_i-\bar{O})^2} \quad (3.10)$$

where, *C* is the Nash-Sutcliffe criterion or coefficient of efficiency, *O* and *M* are the observed and modeled I_c, respectively, and $\bar{O}$ is the mean observed I_c.

RESULTS

Plot-Scale Canopy Water Balance

During the study period precipitation fell in the form of rainfall and as mixed rain-snow events. However, only rainfall events were considered for this study (n = 39). Data for one of these events was not collected since the instrumentation at the plot was temporarily removed due to the close proximity of a forest wildfire. For the remaining 38 events the cumulative rainfall was 252.9 mm (mean = 6.7 mm, median = 5.4 mm), with individual events ranging from 0.5 to 30.8 mm. Forty-seven percent of rainfall events had associated depths < 5.0 mm, while those events with depths > 10.0 mm accounted for 18% of events. Although a relatively small fraction of the number of events, large storms (> 10 mm) accounted for ~ 52% of the cumulative rainfall. Throughfall, stemflow and I_c, totaled 221.9, 4.5, and 26.5 mm accounting for 87.7, 1.8 and 10.5 percent of the rainfall, respectively.

The relationships between event rainfall depth (mm) and the depths (mm) associated with each of the canopy water fluxes were found to be linear (Figure 3.7a and 3.7b):

$$TF = 0.917\,Pg - 0.278, r^2 = 0.99,\ n = 38 \quad (3.11)$$

$$SF = 0.021\,Pg - 0.016, r^2 = 0.83, n = 38 \quad (3.12)$$

$$Ic = 0.062\,Pg + 0.302, r^2 = 0.59,\ n = 38 \quad (3.13)$$

where, *TF* and *SF* are throughfall (mm) and stemflow (mm), respectively, while P_g represents rainfall depth (mm).

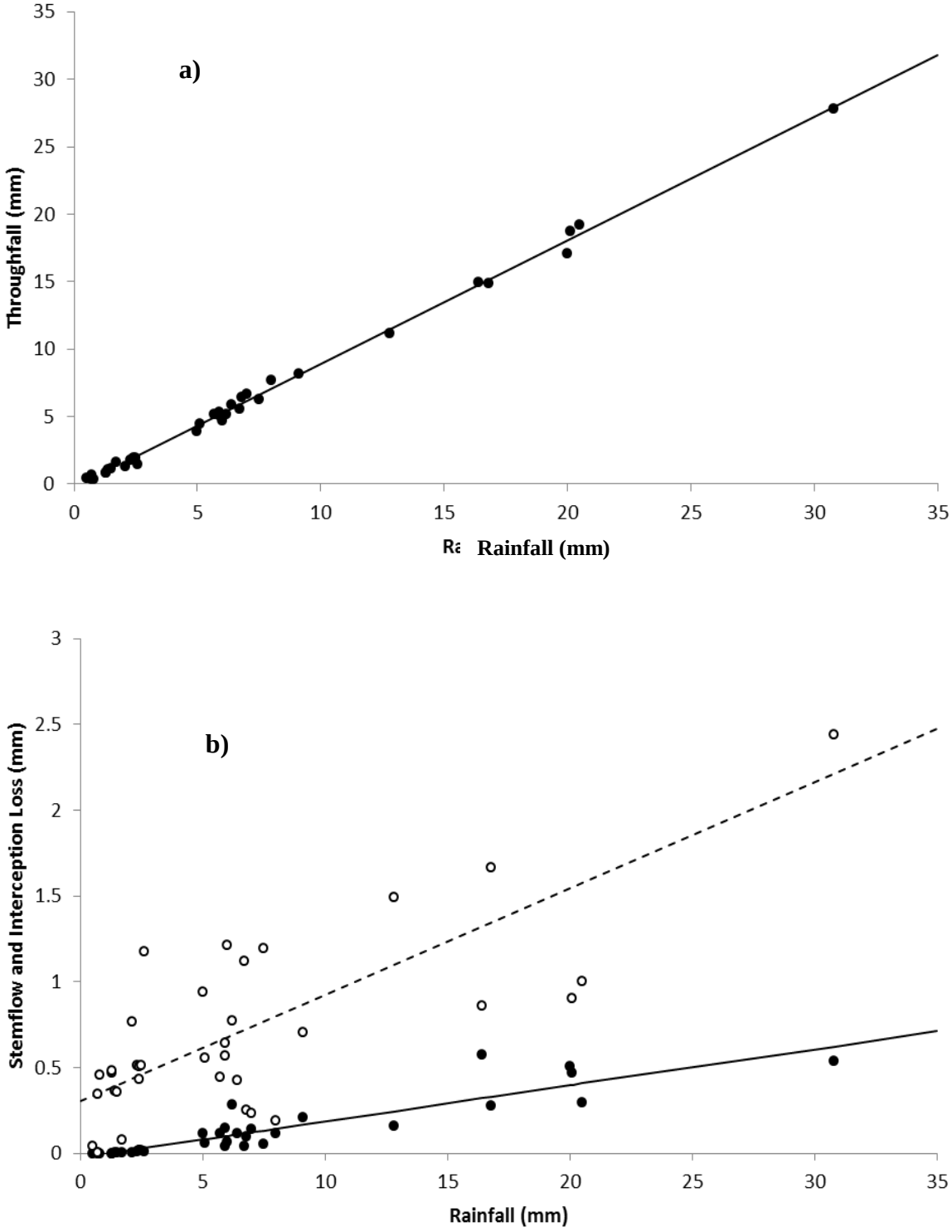

Figure 3.7: a) Event throughfall and **b**) event stemflow (mm) ─●─ and interception loss (mm) ---○--- versus rainfall (mm).

The proportion of rainfall that became throughfall and stemflow increased, while the proportion of rainfall that became interception loss decreased with increasing rainfall depth (Table 3.2).

Table 3.2: Percentage of rainfall partitioned into throughfall, stemflow and canopy interception loss for four rainfall depth classes.

Rainfall Class (mm)	***TF* (%)**	***SF*(%)**	***Ic* (%)**
≤1.5	70.3	0.1	29.6
1.6 – 4.9	75.6	0.4	24.0
5.0 – 9.9	87.7	1.8	10.5
≥10	89.9	2.1	8.0

Modeling Results

The derived parameter values for both the Gash and Liu models are provided in Table 3.3. The Gash and Liu models estimated cumulative *Ic* at 24.7 and 24.6 mm (9.8% and 9.7% of rainfall), respectively, compared with the observed 26.5 mm (10.5% of rainfall); an underestimate of 1.8 and 1.9 mm or 6.8 and 7.2% of the observed *Ic*, respectively. No significant difference ($p < 0.0001$) was found between the slope of the Liu versus Gash modeled results and unity nor was there a significant difference ($p < 0.05$) between the intercept and zero (Figure 3.8).

Table 3.3: Gash and Liu model parameter values derived for the study stand.

Parameter	Value	Description	Model
Sc	0.36	Canopy storage capacity (mm)	Gash, Liu
Ec	0.45	Mean evaporation rate from a saturated canopy (mm h^{-1})	Gash, Liu
R	1.35	Mean rainfall intensity (mm h^{-1})	Gash, Liu
c	0.265	Canopy cover fraction (dimensionless)	Gash, Liu
Stc	0.00	Trunk storage capacity (mm)	Gash, Liu
Pd	0.10	Drainage portioning coefficient (dimensionless)	Gash
ε	0.023	Trunk: Canopy evaporation constant (dimensionless)	Gash
Pg’	0.43	Depth of gross precipitation required to fill canopy storage (mm)	Gash
Pg”	0.43	Depth of gross precipitation required to fill trunk storage (mm)	Gash

Observed and modeled accumulative *Ic* (mm) using the modeling approaches versus accumulative rainfall (mm) is provided in Figure 3.9. The cumulative RMSE and r^2 values for the Gash and Liu modeled event-scale *Ic* versus observed event-scale *Ic* were 0.155 and

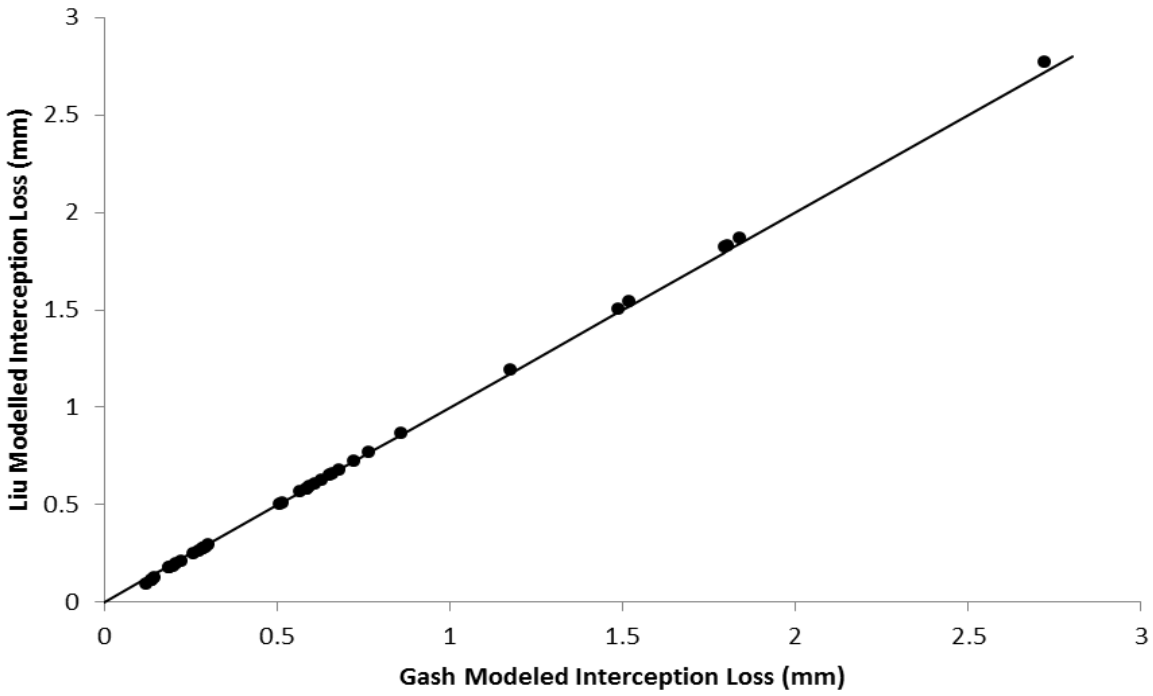

Figure 3.8: Liu modeled interception loss (mm) versus Gash modeled interception loss (mm).

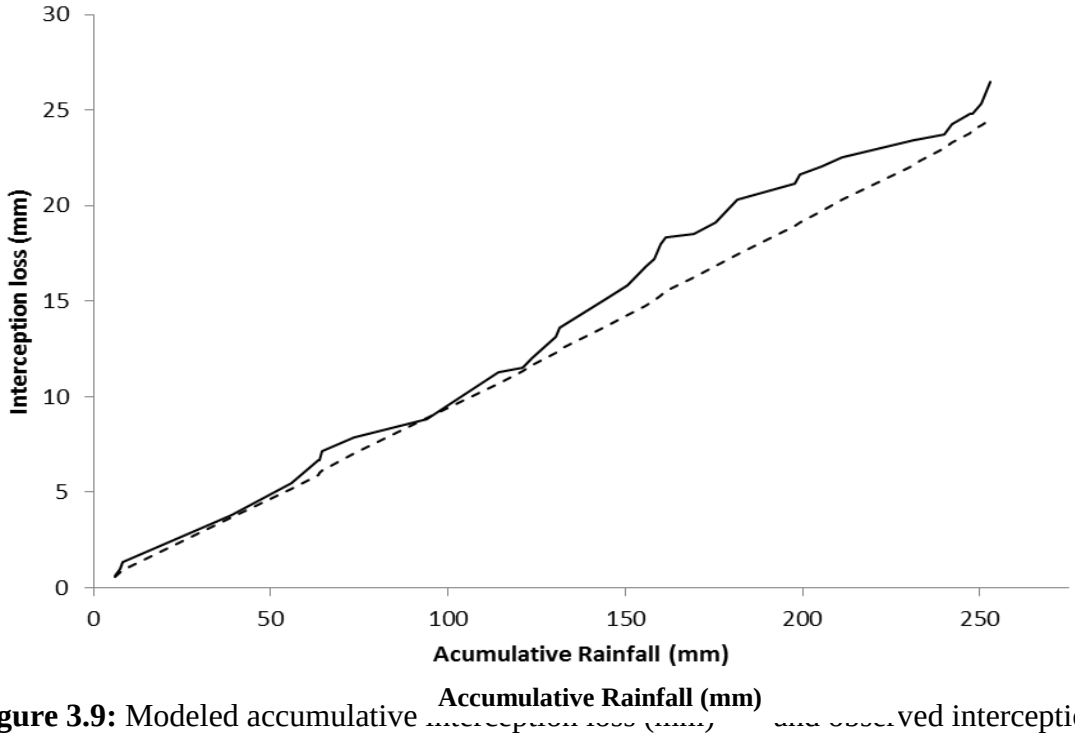

Accumulative Rainfall (mm)

Figure 3.9: Modeled accumulative interception loss (mm) and observed interception loss (mm) as a function of accumulative rainfall (mm).

0.160 mm and 0.586 and 0.587, respectively. The Nash-Sutcliffe criterion value for the Gash model was found to be 0.487, while for the Liu model it was 0.471.

An analysis was completed to determine the Gash and Liu model's sensitivity to changes in parameter values by recording the ratio between the model output compared to the original estimate as a function of the change to the parameter (%) (Figure 3.10).

DISCUSSION AND CONCLUSION

Although the fraction of season-long rainfall portioned into I_c in this juvenile lodgepole pine stand, 10.5%, is similar to that found in other environments where isolated trees dominate (e.g., David *et al*. 2006), it is considerably less than that found for mature lodgepole pine stands and lodgepole pine dominated stands in the region. Carlyle-Moses *et al*. (2014), for example, found that 41% of the rainfall associated with 14 events (total depth = 50.1 mm) during the growing season of 2008 in a mature (125 year-old) declining hybrid white spruce (*Picea glauca* (Moench) Voss × *P. engelmannii* Parry ex Engelm.), subalpine fir (*Abies lasiocarpa* (Hook.) Nutt.), and lodgepole pine (*Pinus contorta* var. *latifolia* Dougl. ex Loud.) forest located approximately 0.85 km NW of the study plot was partitioned into *Ic*. Spittlehouse (1998) found that I_c accounted for 24% of a May to October storm record totaling 454 mm in a mature lodgepole pine dominated forest near Penticton, British Columbia. However, that the magnitude and frequency of rain events play a large role in determining the percentage of rainfall that is partitioned into I_c (Carlyle-Moses and Gash 2011). Using the linear regression relating I_c depth to rainfall depth for the mature spruce-fir-pine stand derived by Carlyle-Moses *et al*. (2014) and the rain record for this current study, approximately 85.3 mm, or 33.7% of the season-long rainfall would have been partitioned into I_c by the mature forest, representing an I_c efficiency approximately 3 times that of the juvenile stand.

Intuitively, the lower I_c efficiency of the juvenile forest compared to that of the mature forest is due, in no small part, to the relatively lower canopy cover fraction, 26.5% compared to 58%. However, the composition of that cover, including the fraction of wood relative to foliage, difference in LAI, the canopy depth, and the presence and abundance of epiphytes, are also likely reasons for the differences in the fractioning of rain into I_c by the

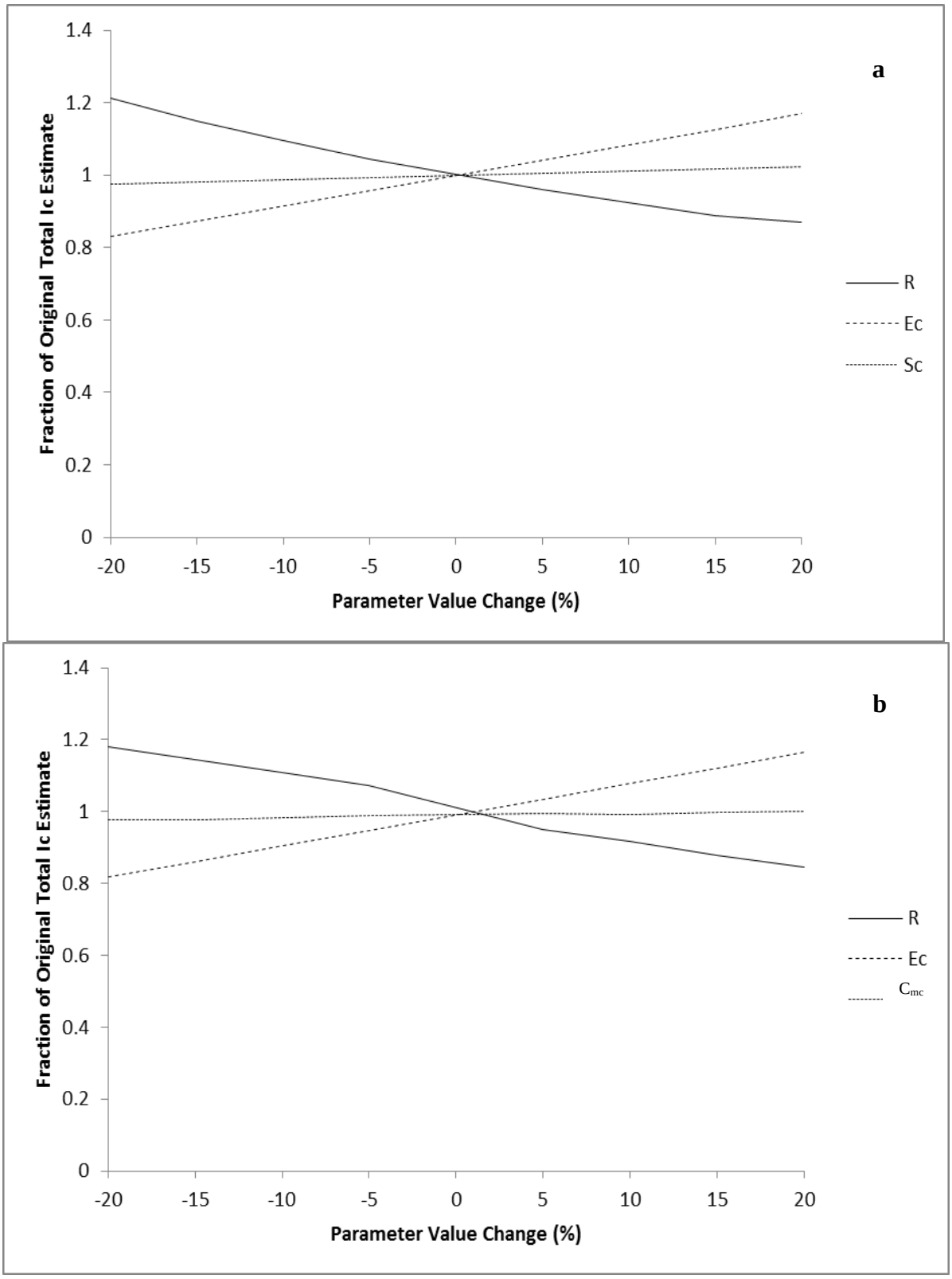

Figure 3.10: Sensitivity of the reformulated Gash (a) and Liu (b) models to changes in model parameter values.

juvenile and mature stands (Spittlehouse, 1998). Carlyle-Moses *et al.* (2007) derived a storage capacity ranging from 2.06 to 3.22 mm on a per unit canopy area basis for the aforementioned mature lodgepole pine dominated stand near Penticton, British Columbia, a full order of magnitude greater than the S_c value derived for the juvenile stand in this current study (0.36 mm). Other studies in mature coniferous forests have also found relatively large S_c values, including 4.47 mm for a *Pinus armandii* in the Ningxia Hui Autonomous Region of China.(Zhongjie *et al*. 2010)

The mean during-event evaporation rate of the juvenile pines (0.45 mm h^{-1}) is well within the range (0.07 to 0.70 mm h^{-1}) reported from other forests (Carlyle-Moses and Price, 2007); however, the juvenile pine E_c value exceeds, albeit only slightly, the bounds of the mean ± standard deviation of 0.3 ± 0.1 mm h^{-1} derived by Miralles *et al*. (2010), which is based on the results of twelve studies conducted using data from forests around the globe. Additionally, E_c for the juvenile stand is within the range derived for the mature lodgepole pine forest near Penticton, British Columbia, 0.44 to 0.77 mm h^{-1} (Carlyle-Moses *et al*. 2007). Thus, the E_c rate found for the juvenile pine stand is relatively high, considering the relative short stature of these trees, compared to the mature stand; a possible consequence of the increased ventilation offered by these relatively isolated trees (Carlyle-Moses *et al*. 2010; Teklehaimanot et al. 1991). However, as David *et al*. (2006) note, stand density or canopy cover may not affect the rate of I_c on a per unit of crown-projected area basis and that the reformulated Gash model (and Liu model) assumes that E decreases linearly with decreasing canopy cover. Nonetheless, I_c is relatively high when expressed on a per canopy cover fraction basis (39.6%) and is due in no small part to the relatively large E_c value derived for this stand.

Very little difference was found between the performance of the reformulated Gash and reformulated Liu models, in keeping with the results of Carlyle-Moses and Price (2007) in a mature pine-oak stand in northeastern Mexico. Error analysis for the current study suggests that both the reformulated Gash and Liu models are particularly sensitive to variations in R and E_c, and much less so for variations in S_c. Similar findings have been found for other forest and plantation environments (e.g., Carlyle-Moses and Price 2007; Carlyle-Moses *et al*. 2010; Muzylo *et al*. 2012). Since, for a given stand, E_c and the ratio of E_c: R varies largely with wind speed and vapour pressure deficit (see Pereira *et al*., 2009;

Carlyle-Moses and Gash, 2011; Llorens, 1998), it is not surprising to find the relatively large errors associated with the two models at the rainfall event scale with both the Gash and Liu models not able to explain approximately 41% of the variation in observed I_c.

In summary, the current study suggests that I_c is more reduced in juvenile stands compared to their mature counterparts and that this reduction is due to the decreased storage capacity offered by these younger canopies. Evaporation during rainfall from juvenile canopies is still appreciable and may be a consequence of the increased proportion of the canopy exposed to wind during events. The partitioning of water by the canopies of these juveniles stands also differs from mature forests in that stemflow represents a greater proportion of total rainfall than it does in older stands.

Although the fraction of rainfall partitioned by the canopy is still small, representing less than 2% over the study period, the concentrated input of this water (see Mckee and Carlyle-Moses 2010) may have important implications for site hydrology that remain to be explored. Additionally, the fate of the increased input of total canopy drainage (throughfall + stemflow), which is approximately is estimated to be 15 to 20% of growing-season rainfall, on the hydrology of these juvenile forests and how this compares with the water stores and fluxes in mature stands also requires further study.

REFERENCES

Aston AR. 1979. Rainfall interception by eight small trees. *Journal of Hydrology* **42**: 383–396.

B.C. Ministry of Forests and Range. 2008. Biogeoclimatic ecosystem classification subzone/variant map for the Arrow Boundary Forest District, Boundary Subunit, Southern Interior Forest Region. 1:250 000. Research Branch, Victoria, B.C.

Calder, IR. 1990. Evaporation in the uplands. John Wiley & Sons Ltd., Chichester, 166 p.

Carlyle-Moses DE, Lishman CE, McKee AJ. 2014. A preliminary evaluation of throughfall sampling techniques in a mature coniferous forest. *Journal of Forestry Research* **25**: 407-413

Carlyle-Moses DE, Gash JHC. 2011. Rainfall Interception Loss by Forest Canopies. In: *Forest Hydrology and Biogeochemistry: Synthesis of Past Research and Future Directions*, Levia DF, Carlyle-Moses DE, Tanaka T (eds.). *Ecological Series* **216**, Springer-Verlag: Heidelberg, Germany; 407-423

Carlyle-Moses DE, Park AD, Cameron JL. 2010. Modelling rainfall interception loss in forest restoration trials in Panama. *Ecohydrology* **3**: 272-283

Carlyle-Moses DE, Price AG. 2007. Modelling canopy interception loss from a Madrean pine-oak stand, Northeastern Mexico. *Hydrological Processes* **21**: 2572-2580

Carlyle-Moses DE, Schimpf GR and DL Spittlehouse. 2007. "Influence of rainfall event separation time on the analytical modelling of canopy interception loss from a mature lodgepole pine (*Pinus contorta* var. *latifolia*) stand" In: Program and Abstracts of the Joint Canadian Meteorological and Oceanographic Society, the Canadian Geophysical Union, and the American Meteorological Society Annual Meetings, St. John's, Newfoundland, Canada, 28 May –1 June.

Coops, NC, Waring, RH, Wulder, MA, White, JC. 2009. Prediction and assessment of bark beetle-induced mortality of lodgepole pine using estimates of stand vigour derived from remotely sensed data. *Remote Sensing of Environment.* **113:** 1058-1066

Dhar A, Wang JR, Hawkins CDB. 2015. Interaction of Trembling Aspen and Lodgepole Pine in a Young Sub-Boreal Mixedwood Stand in Cnetral British Columbia. Open Journal of Forestry **5:** 129-138.

David TS, Gash JHC, Valente F, Pereira JS, Ferreira MI, David JS. 2006. Rainfall interception by an isolated evergreen oak tree in a Mediterranean savannah. *Hydrological Processes* **20**: 2713-2726

Gash JHC. 1979. An analytical model of rainfall interception in forests. *Quarterly Journal of the Royal Meteorological Society* **105**: 43-55

Gash JHC, Lolyd CR, Lachaud G. 1995. Estimating sparse forest rainfall interception with an analytical model. *Journal of Hydrology* **170:** 79-86

Helvey JD, Patric JH. 1965. Canopy and litter interception of rainfall by hardwoods of eastern United States. *Water Resources Research* **1**: 193-206

Klaassen, W, Bosveld, F, Water, E (1998) Water storage and evaporation as constitutes of rainfall interception. *Journal of Hydrology* **212–213**: 36-50

Ladson A. 2008. Hydrology: An Australian introduction. Oxford University Press. New York

Liu S. 1997. A new model for the prediction of rainfall interception in forest canopies. *Ecological Modeling* **99**: 151-159

Liu S. 2001. Evaluation of the Liu model for predicting rainfall interception in forests world-wide. *Hydrological Processes* **15**: 2341-2360

Llorens P. 1998. Rainfall interception by a Pinus sylvestris forest patch overgrown in a Mediterranean mountainous abandoned area II. Assessment of the applicability of Gash's analytical model. *Journal of Hydrology* **199**: 346-359.

Mayer DG. And Butler DG. 1993. Statistical validation. *Ecological Modelling* **68**: 21-32

McKee A ,Carlyle-Moses DE. 2010. Stemflow: A potentially important point source of water for growth. *FORREX Forum for Research and Extension in Natural Resources:*11-12

Miralles DG, Gash JH, Holmes TRH, de Jeu RAM and AJ Dolman. Global canopy interception from satellite observations. *Journal of Geophysical Research* **115:** Di6122

Moore, RD, Winkler, RD, Carlyle-Moses, DE. 2008. Watershed response to the McLure forest fire: presentation summaries from the Fishtrap Creek workshop, March 2008. *Streamline Watershed Manage Bulletin* **12**: 1-11

Muzylo A, Llorens P., Valente F., Keizer J.J., Domingo D, and Gash J.H.C. 2009. A review of rainfall interception modelling. *Journal of Hydrology* **370**: 191–206

Pereira FL, Gash JHC, David JS, David TS, Monteiro PR and F Valente. 2009. Modelling interception loss from evergreen oak Mediterranean savannas: Application of a tree-based modelling approach. *Agricultural and Forest Meteorology* **149**: 680-688

Price AG, Carlyle-Moses DE. 2003. Measurement and modelling of growing-season canopy water fluxes in mature mixed deciduous forest stand, southern Ontario, Canada. *Agricultural and Forest Meteorology* **119**: 69-85

Rice AV, Thormann MN, Langor DW. 2007. Mountain pine beetle associated blue-stain fungi cause lesions on jack pine, lodgepole pine, and lodgepole x jack pine hybrids in Alberta. *Canadian Journal of Botany* **85**: 307-315

Roth, BE, Slatton, KC, Cohen, MJ. 2007. On the potential for high-resolution lidar to improve rainfall interception estimates in forest ecosystems. *Frontiers in Ecology and the Environment* **5**: 421-428

Rutter, AJ, Kershaw, KA, Robins, PC. 1971. A predictive model of rainfall interception in forests I: derivation of the model from observations in a plantation of Corsican pine. *Agricultural Meteorology* **9**: 367-384

Rutter, A, Morton, A. Robin, P., 1975. A Predictive Model of Rainfall Interception in Forests. II. Generalization of the Model and Comparison with Observations in Some Coniferous and Hardwood Stands. *Journal of Applied Ecology* **12**: 367–380

Spittlehouse DL. 1998. Rainfall interception in young and mature conifer forests in British Columbia. *Proceedings of the 23rd Conference on Agricultural and Forest*

Meteorology, 2-6 November 1998, Albuquerque, New Mexico: American Meteorological Society.

Teklehaimanot, Z, Jarvis, PG. 1991. Rainfall interception and boundary layer conductance in relation to tree spacing. Journal of Hydrology **123**: 261-278

Valente, F., David, J.S., Gash, J.H.C., 1997. Modelling interception loss for two sparse eucalypt and pine forests in central Portugal using reformulated Rutter and Gash analytical models. *Journal of Hydrology* **190**: 141–162

Winkler RD, Boon S, Zimonick B, Baleshta K. 2010. Assessing the effects of post-pine beetle forest litter on snow albedo. *Hydrological Processes* **24**:803–812

Zhongjie S, Yanhui W, Lihong X, Pentao Y, Jixi G and Z Linbo. 2010. Fraction of incident rainfall within the canopy of a pure stand of *Pinus armandii* with revised Gash model in the Liupan Mountains of China. *Journal of Hydrology* **385**: 44-50

CHAPTER 4
CONCLUSION

A juvenile lodgepole pine (*Pinus contorta* Douglas ex Louden var. *latifolia* Engelm. ex S. Watson) stand in south-central British Columbia was examined, in order to determine the magnitude of point and structural *TF* as well as *SF* at the rainfall event and growing-season temporal scales. Chapter 2 evaluated if *TF* (both point and structural) and *SF* spatial variability exhibits temporal persistence and if so to determine what the influence, if any, certain tree and storm characteristics may have on this stability. The present study has found that TF is modified by the canopies of juvenile lodgepole pine in a systematic fashion, with this understory precipitation input typically increasing and its associated spatial heterogeneity decreasing with increasing distance from the tree bole. Tree and storm characteristics, such as tree size and direction of storm origin, were found to explain some of the variability in the spatial delivery of TF, however, the role of other variables that are likely drivers of this variability in this forest type, including wind speed and direction as well as wood cover, still need to be assessed. The spatial variability of TF exhibits temporal persistence that marginally degrades with time across the study period, probably as a result of slight changes to the canopy during growth across the time span of the study (five months). Temporal persistence was also found to degrade as a consequence of differences in the certain meteorological characteristics, such as the 30-minute rain intensity, suggesting that alike storms produce alike TF spatial patterns. However, it is not clear why differences in intra-storm break duration and or number of breaks among events resulted in a strengthening of persistence. Nonetheless, much of the variability in the persistence of TF spatial patterns from one event to the next in this study was not explained. Again, wind speed and direction may be important factors that required future study.

Finally, Chapter 2 provided some recommendations for sampling strategies for future research in similar forests environments. Our results suggest that future TF sampling in these juvenile forests be done with relatively denser networks of TF gauges in the inner- and mid-canopy zones as compared with the canopy-periphery and areas outside of the canopy due to the increased TF variability observed in the former zones. Areas outside of the canopy, however, are still influenced by the canopies of juvenile pine, probably as a result of the

effective catch of inclined rainfall, and thus still need to be sampled. The prevailing direction of storm origin should also be considered when establishing TF sampling networks.

Chapter 3 dealt with interception modelling, specifically to evaluate the performance of the reformulated Gash (Valente *et al*., 1997) and reformulated Liu (Carlyle-Moses and Price, 2007) I_c models at both event and season-long time scales, as well as to determine the quantitative importance of throughfall, stemflow and I_c. Furthermore, this chapter assessed if the data collected supports a 'water-box' or an 'exponential wetting approach' of the canopy saturation process. The current study suggests that I_c is more reduced in juvenile stands compared to mature stands and that this reduction is due to the decreased storage capacity offered by these younger canopies. Evaporation during rainfall from juvenile canopies is still appreciable and may be a consequence of the increased proportion of the canopy exposed to wind during events.

LIMITATIONS

The initially proposed thesis involved every aspect of forest hydrology, ranging from measuring rainfall, throughfall (5472 TF points), stemflow (239 +516), soil moisture content (4224 TDR points), meteorological station data, infiltration rates (96 minidisk infiltrometers tests), macropore study using urinine tracer dye (15 tracer dye experiments) as well as measuring groundwater levels (two monitoring wells). The sum of these measured forest hydrology parameters resulted in tens of thousands of data points, which proved to be overwhelming for the scope of the MSc. Thesis. All the data was collected for the above mentioned parameters of forest hydrology, however only throughfall, stemflow and rainfall data were analyzed during this study.

Due to the sheer scope of the research project, logistical and financial restraints reduced the number of plots to create the dataset required for developing the interception models, and to determine the magnitude of point and structural *TF* as well as *SF* at the rainfall event and growing-season temporal scales. Additionally, *TF* (both point and structural) spatial variability was evaluated to determine if it exhibited temporal persistence at only one plot.

The inclusion of more samples from other similar aged tree stand locations would have resulted in more comprehensive interception models which could be compared to one another.

APPLICATION OF RESEARCH

One possible practicable application of Chapter 3 can be to help provide accurate interception modelling data for the proposed BC Water Development Tool, which is based off of the Oil and Gas Commission NorthEast Water Tool (NEWT, 2015). NEWT uses gridded climate, topography and land cover information to develop a simple water balance model (Q=P-ET). As these GIS tools evolve and become more in-depth, interception models can be used in conjunction with forest land cover to provide more accurate and area specific interception and evapotranspiration values. Additionally, interception loss and SF funnelling ratios can be used to further our ability to predict flooding, better control of water allocation for agricultural purposes and to provide more regulated surface water runoff control in forested and cut-block areas.

FUTURE STUDY DIRECTIONS

Tree and storm characteristics, such as tree size and direction of storm origin, were found to explain some of the variability in the spatial delivery of TF, however, the role of other variables that are likely drivers of this heterogeneity in this forest type, including wind speed and direction as well as wood cover, still needs to be addressed.

The systematic nature of the spatial heterogeneity of TF and its temporal persistence suggests that directly or indirectly TF influenced hydrological, biogeochemical, and ecological aspects of these young forests may also have associated spatiotemporal trends. Further study to establish if such linkages exist is required. Additionally, spatiotemporal patterns in TF and associated hydroecological processes, if they exist, should be assessed at different stages of growth so that the impact of forest disturbance regimes, such as the mountain pine beetle, and subsequent re-growth may be better understood.

The partitioning of water by the canopies of these juveniles stands also differs from mature forests. Based on the results of this current study in a juvenile lodgepole pine forests and the results of past studies in mature lodgepole pine forests, it may be expected that interception

loss will increase while throughfall and stemflow will decrease as the stand ages (Figure 4.1). This is owed to an increase in storage capacity as the tree ages, primarily to the relatively higher canopy cover fraction of the mature stand, as well as thicker and coarser bark (Carlyle-Moses *et al.*2007). Because of the dependence of evaporation and storage capacity on meteorological conditions, further study is needed, especially studies in which interception loss, thoughfall and stemflow are measured over a chronosequence of stands of varying ages under the same meteorological conditions so that the role of canopy characteristics can truly be identified.

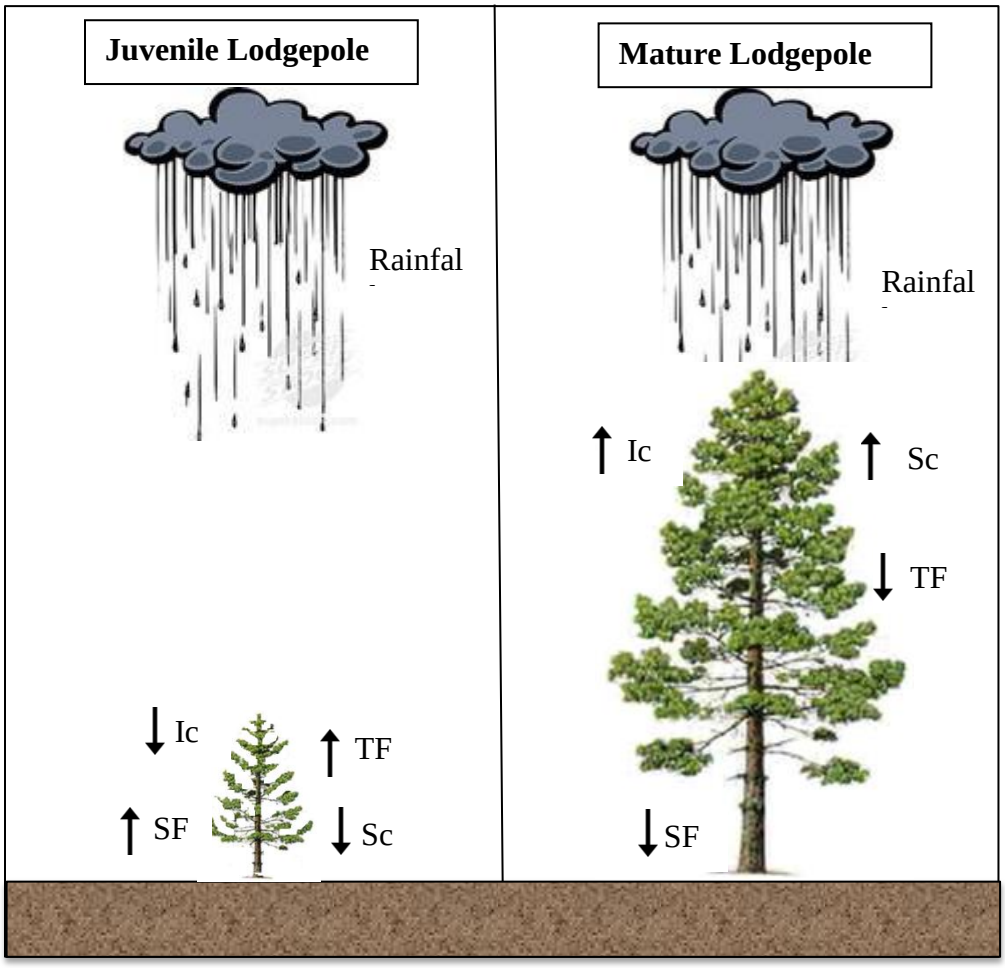

Figure 4.1: Conceptual model comparing a juvenile and mature lodgepole pine tree rainfall partitioning.

Even though the fraction of rainfall partitioned by the canopy is small, representing less than 2% over the study period, the concentrated input of this water (see McKee and

Carlyle-Moses 2010) may have important implications for site hydrology that remain to be explored. Additionally, the fate of the increased input of total canopy drainage (throughfall + stemflow), which is approximately 15 to 20% of growing-season rainfall, on the hydrology of these juvenile forests and how this compares with the water stores and fluxes in mature stands also requires further study.

REFERENCES

BC Oil and Gas Commission. 2015. Northeast Water Tool. Retrieved from http://geoweb.bcogc.ca/apps/newt/newt.html

Carlyle-Moses DE, Price AG. 2007. Modelling canopy interception loss from a Madrean pine-oak stand, Northeastern Mexico. *Hydrological Processes* **21**: 2572-2580

Carlyle-Moses DE, Schimpf GR , DL Spittlehouse. 2007. "Influence of rainfall event separation time on the analytical modelling of canopy interception loss from a mature lodgepole pine (*Pinus contorta* var. *latifolia*) stand" In: Program and Abstracts of the Joint Canadian Meteorological and Oceanographic Society, the Canadian Geophysical Union, and the American Meteorological Society Annual Meetings, St. John's, Newfoundland, Canada, 28 May –1 June.

McKee A, Carlyle-Moses D. 2010. Stemflow: A potentially important point source of water for growth. *FORREX Forum for Research and Extension in Natural Resources:* 11-12

Valente, F., David, JS, Gash, JHC. 1997. Modelling interception loss for two sparse eucalyptus and pine forests in central Portugal using reformulated Rutter and Gash analytical models. *Journal of Hydrology* **190:** 141–162